

1 **Answer to Editor Prof. Appy Sluijs**

2 Thanks to Editor for his comments and suggestions referring the manuscript CP-2015-113  
3 entitled "Palaeoclimatic oscillations in the Pliensbachian (Lower Jurassic) of the Asturian Basin  
4 (Northern Spain)". Together with the valuable comments and suggestions received from the  
5 three anonymous referees, have contributed to substantial improvement of the manuscript.

6 At this respect, attached please find two documents of the text. The "Gomez et al TEXT  
7 Corrected\_3" and the "Gomez et al TEXT Corrected Changes Marked\_3". The first .pdf file  
8 contains the text, after corrections, and in the second .doc file highlights, marked in red colour;  
9 the changes introduced from Referees 1 and 2 and in blue colour the changes indicated by  
10 Referee 3, respect to the previous text.

11 All the parts concerning the possible presence of ice caps during the Pliensbachian Cooling  
12 Interval have been deleted from previous versions of the manuscript.

13 We assume that all the requirements pointed by Editor and Referees have been accomplished,  
14 but if any additional modification or clarification is required please do not hesitate to contact  
15 us at your earliest convenience.

16 We are looking forward to receiving your opinion on the revised manuscript.

17 Sincerely,

18 Juan J. Gómez

19

20 **Palaeoclimatic oscillations in the Pliensbachian (Early Jurassic) of the Asturian Basin**  
21 **(Northern Spain).**

22 J.J. Gómez<sup>1</sup>, M.J. Comas-Rengifo<sup>2</sup> and A. Goy<sup>3</sup>

23

24 <sup>1</sup> Departamento de Estratigrafía, Facultad de Ciencias Geológicas (UCM) and Instituto de  
25 Geociencias (CSIC-UCM). 28040 Madrid. Spain

26 <sup>2</sup> Departamento de Paleontología, Facultad de Ciencias Geológicas (UCM). 28040  
27 Madrid. Spain

28 <sup>3</sup> Departamento de Paleontología, Facultad de Ciencias Geológicas (UCM) and Instituto  
29 de Geociencias (CSIC-UCM). 28040 Madrid. Spain

30

31 *Correspondence to:* [jgomez@ucm.es](mailto:jgomez@ucm.es)

32

33 **Abstract.**

34 **One of the main controversial items in palaeoclimatology is to elucidate if climate**  
35 **during the Jurassic was warmer than present day and equal over Pangea, with no**  
36 **major latitudinal gradients. Abundant evidences of oscillations in seawater**

37 temperature through the Jurassic have been presented. The Pliensbachian (Early  
38 Jurassic) is a singular time interval on which several seawater temperature oscillations  
39 are documented in this work, including an exceptional cooling event. To constrain the  
40 timing and magnitude of these climate changes, the Rodiles section of the Asturian  
41 Basin (Northern Spain), a well exposed succession of the uppermost Sinemurian,  
42 Pliensbachian and Lower Toarcian deposits, has been studied. A total of 562 beds were  
43 measured and sampled for ammonites, for biochronostratigraphical purposes, and for  
44 belemnites, to determine the palaeoclimatic evolution through stable isotope studies.  
45 Comparison of the recorded latest Sinemurian, Pliensbachian and Early Toarcian  
46 changes in seawater palaeotemperature with other European sections allows  
47 characterization of several climatic changes of probable global extent. A warming  
48 interval which partly coincides with a  $\delta^{13}\text{C}_{\text{bel}}$  negative excursion was recorded at the  
49 Late Sinemurian. After a “normal” temperature interval, a new warming interval that  
50 contains a short lived positive  $\delta^{13}\text{C}_{\text{bel}}$  peak, was developed at the Early–Late  
51 Pliensbachian transition. The Late Pliensbachian represents an outstanding cooling  
52 interval containing a  $\delta^{13}\text{C}_{\text{bel}}$  positive excursion interrupted by a small negative  $\delta^{13}\text{C}_{\text{bel}}$   
53 peak. Finally, the Early Toarcian represented an exceptional warming period pointed as  
54 the main responsible for the prominent Early Toarcian mass extinction.

55

## 56 1 Introduction

57 The idea of an equable Jurassic greenhouse climate, 5–10° C warmer than present day,  
58 with no ice caps and low pole-equator temperature gradient, has been proposed by  
59 several studies (i.e. Hallam, 1975, 1993; Chandler et al., 1992; Frakes et al., 1992; Rees  
60 et al., 1999). Nevertheless, this hypothesis has been challenged by numerous  
61 palaeoclimatic studies, mainly based on palaeotemperature calculations using the  
62 oxygen isotope data from belemnite and brachiopod calcite as a proxy.

63 Especially relevant are the latest Pliensbachian–Early Toarcian climate changes, which  
64 have been documented in many sections from Western Europe (i. e. Sælen et al., 1996;  
65 McArthur et al., 2000; Röhl et al., 2001; Schmidt-Röhl et al., 2002; Bailey et al., 2003;  
66 Jenkyns, 2003; Rosales et al., 2004; Gómez et al., 2008; Metodiev and Koleva-Rekalova,  
67 2008; Suan et al., 2008, 2010; Dera et al., 2009, 2010, 2011; Gómez and Arias, 2010;  
68 García Joral et al., 2011; Gómez and Goy, 2011; Fraguas et al., 2012), as well as in  
69 Northern Siberia and in the Arctic Region (Zakharov et al., 2006; Nikitenko, 2008; Suan  
70 et al., 2011). The close correlation between the severe Late Pliensbachian Cooling and  
71 the Early Toarcian Warming events, and the major Early Toarcian mass extinction  
72 indicates that warming was one of the main causes of the faunal turnover (Kemp et al.,  
73 2005; Gómez et al., 2008; Gómez and Arias, 2010; García Joral et al., 2011; Gómez and  
74 Goy, 2011; Fraguas et al., 2012; Clémence, 2014; Clémence et al., 2015; Baeza-  
75 Carratalá et al., 2015).

76 Nevertheless, except for a few sections (Rosales et al., 2004; Korte and Hesselbo, 2011;  
77 Suan et al., 208, 2010), little data on the evolution of seawater palaeotemperatures  
78 during the latest Sinemurian and the Pliensbachian have been published, even some  
79 more papers studied the climatic changes of parts of the considered time interval (i.e.

80 McArthur et al., 2000; Hesselbo et al., 2000; Jenkyns et al., 2002; van de Scootbrugge  
81 et al., 2010; Gómez and Goy, 2011; Armendariz et al., 2012; Harazim et al., 2013).

82 The objective of this paper is to provide data on the evolution of the seawater  
83 palaeotemperatures and the changes in the carbon isotopes through the **Late**  
84 **Sinemurian**, **Pliensbachian** and **Early Toarcian (Early Jurassic)** and to constrain the  
85 timing of the recorded changes through ammonite-based biochronostratigraphy. The  
86 dataset has been obtained from the particularly well exposed Rodiles section, located  
87 in the Asturias community in Northern Spain (Fig. 1). **Results have been correlated with**  
88 **the records obtained in different sections of Europe, showing that these climatic**  
89 **changes, as well as the documented perturbations of the carbon cycle, could be of**  
90 **global, or at least of regional extent at the European scale.**

91

## 92 **2 Materials and methods**

93 The 110 m thick studied section composed of 562 beds has been studied bed by bed.  
94 Collected ammonites were prepared and studied following the usual palaeontological  
95 methods. The obtained biochronostratigraphy allowed characterization of the  
96 standard chronozones and subchronozones established by Elmi et al. (1997) and Page  
97 (2003), which are used in this work.

98 A total of 191 analyses of stable isotopes were performed on **163** belemnite calcite  
99 samples, in order to obtain the primary **Late Sinemurian**, **Pliensbachian** and **Early**  
100 **Toarcian** seawater stable isotope signal, and hence to determine palaeotemperature  
101 changes, as well as the variation pattern of the carbon isotope in the studied time  
102 interval. For the assessment of possible burial diagenetic alteration of the belemnites,  
103 polished samples and thick sections of each belemnite rostrum were prepared. The  
104 thick sections were studied under the petrographic and the cathodoluminescence  
105 microscope, and only the non-luminescent, diagenetically unaltered portions of the  
106 belemnite **rostrum**, were sampled using a microscope-mounted dental drill.  
107 **Belemnites in the Rodiles section generally show an excellent degree of preservation**  
108 **(Fig. 2) and none of the prepared samples were rejected, as only the parts of the**  
109 **belemnite rostrum not affected by diagenesis were selected.** Sampling of the  
110 luminescent parts such as the apical line and the outer and inner rostrum wall,  
111 fractures, stylolites and borings **were** avoided. Belemnite calcite was processed in the  
112 stable isotope labs of the Michigan University (USA), **using a Finnigan MAT 253 triple**  
113 **collector isotope ratio mass spectrometer.** The procedure followed in the stable  
114 isotope analysis has been described in Gómez and Goy (2011). Isotope ratios are  
115 reported in per mil relative to the standard Peedee belemnite (PDB), having a  
116 reproducibility better than 0.02 ‰ PDB for  $\delta^{13}\text{C}$  and better than 0.06 ‰ PDB for  $\delta^{18}\text{O}$ .

117 The seawater palaeotemperature recorded in the oxygen isotopes of the studied  
118 belemnite rostra have been calculated using the Anderson and Arthur (1983) equation:  
119  $T(^{\circ}\text{C}) = 16.0 - 4.14 (\delta_{\text{c}} - \delta_{\text{w}}) + 0.13 (\delta_{\text{c}} - \delta_{\text{w}})^2$  where  $\delta_{\text{c}} = \delta^{18}\text{O}$  PDB is the composition of the  
120 sample, and  $\delta_{\text{w}} = \delta^{18}\text{O}$  SMOW the composition of ambient seawater. **According to the**  
121 **recommendations of Shackleton and Kennett (1975), the standard value of  $\delta_{\text{w}} = -1\text{‰}$**   
122 **was used for palaeotemperature calculations under non-glacial ocean water**

123 conditions. If the presence of permanent ice caps in the poles is demonstrated for  
124 some of the studied intervals, value of  $\delta_w=0\text{‰}$  would be used and consequently  
125 calculated palaeotemperatures would increase in the order of 4°C.

126 For palaeotemperature calculation, it has been assumed that the  $\delta^{18}\text{O}$  values, and  
127 consequently the resultant curve, essentially reflects changes in environmental  
128 parameters (Sælen et al., 1996; Bettencourt and Guerra, 1999; McArthur et al., 2007;  
129 Price et al., 2009; Rexfort and Mutterlose, 2009; Benito and Reolid, 2012; Li et al.,  
130 2012; Harazim et al., 2013; Ullmann et al., 2014, Ullmann and Korte, 2015), as the  
131 sampled non-luminescent biogenic calcite of the studied belemnite rostra precipitated  
132 in equilibrium with the seawater. It has also being assumed that the biogenic calcite  
133 retains the primary isotopic composition of the seawater and that the belemnite  
134 migration, skeletal growth, the sampling bias, and the vital effects are not the main  
135 factors responsible for the obtained variations. Cross-plot of the  $\delta^{18}\text{O}$  against the  $\delta^{13}\text{C}$   
136 values (Fig. 3) reveals a cluster type of distribution, showing a negative correlation  
137 coefficient ( $-0.2$ ) and very low covariance ( $R^2=0.04$ ), supporting the lack of diagenetic  
138 overprints in the analyzed diagenetically screened belemnite calcite.

139

### 140 **3 Results**

141 In the coastal cliffs located northeast of the Villaviciosa village, in the eastern part of  
142 the Asturias community (Northern Spain) (Fig. 1), the well exposed Upper Sinemurian,  
143 Pliensbachian and Lower Toarcian deposits are represented by a succession of  
144 alternating lime mudstone to bioclastic wackestone and marls with interbedded black  
145 shales belonging to the Santa Mera Member of the Rodiles Formation (Valenzuela,  
146 1988) (Fig. 4). The uppermost Sinemurian and Pliensbachian deposits have been  
147 studied in the eastern part of the Rodiles Cape and the uppermost Pliensbachian and  
148 Lower Toarcian in the western part of the Rodiles Cape (West Rodiles section of Gómez  
149 et al., 2008; Gómez and Goy 2011). Both fragments of the section are referred here as  
150 the Rodiles section (lat. 43°32'22" long. 5°22'22"). Palaeogeographical reconstruction  
151 based on comprehensive palaeomagnetic data, carried out by Osete et al. (2010),  
152 locates the studied Rodiles section at a latitude of about 32° N for the  
153 Hettangian–Sinemurian interval and at a latitude of almost 40° N (the current latitude  
154 of Madrid) for the Toarcian–Aalenian interval.

155 Ammonite taxa distribution and profiles of the  $\delta^{18}\text{O}_{\text{bel}}$ ,  $\delta^{13}\text{C}_{\text{bel}}$  and  $\delta^{13}\text{C}_{\text{bulk}}$  values  
156 obtained from belemnite calcite have been plotted against the 562 measured beds of  
157 the Rodiles section (Fig. 5).

#### 158 **3.1 Lithology**

159 The Upper Sinemurian, Pliensbachian and Lower Toarcian deposits of the Rodiles  
160 section are constituted by couplets of bioclastic lime mudstone to wackestone  
161 limestone and marls. Occasionally the limestones contain bioclastic packstone facies  
162 concentrated in rills. Limestones, generally recrystallized to microsparite, are  
163 commonly well stratified in beds whose continuity can be followed at the outcrop  
164 scale, as well as in outcrops several kilometres apart. However, nodular limestone  
165 layers, discontinuous at the outcrop scale, are also present. The base of some

166 carbonates can be slightly erosive, and they are commonly bioturbated, to reach the  
167 homogenization stage. Ichnofossils, specially *Thalassinoides*, *Chondrites* and  
168 *Phymatoderma*, are also present. Marls, with CaCO<sub>3</sub> content generally lower than 20%  
169 (Bádenas et al., 2009, 2012), are frequently gray coloured, occasionally light gray due  
170 to the higher proportion of carbonates, with interbedded black intervals. **Locally** brown  
171 coloured sediments, more often in the Upper Sinemurian, are present.

### 172 **3.2 Biochronostratigraphy**

173 The ammonite-based biochronostratigraphy of these deposits in Asturias have been  
174 carried out by Suárez-Vega (1974), and the uppermost Pliensbachian and Toarcian  
175 ammonites by Gómez et al. (2008), and by Goy et al. (2010 a, b). Preliminary  
176 biochronostratigraphy of the Late Sinemurian and the Pliensbachian in some sections  
177 of the Asturian Basin has been reported by Comas-Rengifo and Goy (2010), **and the**  
178 **result of more than ten years of bed by bed sampling of ammonites in the Rodiles**  
179 **section, which allowed precise time constrain for the climatic events described in this**  
180 **work, are here summarized.**

181 Collected ammonites allowed the recognition of all the standard **Late** Sinemurian,  
182 Pliensbachian and **Early** Toarcian chronozones and subchronozones defined by Elmi et  
183 al. (1997) and Page (2003) for Europe. Section is generally expanded and ammonites  
184 are common enough as to constrain the boundaries of the biochronostratigraphical  
185 units. Exceptions are the Taylori–Polymorphus subchronozones that could not be  
186 separated, and the Capricornus–Figulinum subchronozones of the Davoei Chronozone,  
187 partly due to the relatively condensed character of this Chronozone. Most of the  
188 recorded species belong to the NW Europe province but some representatives of the  
189 Tethysian Realm are also present.

### 190 **3.3 Carbon isotopes**

191 The carbon isotopes curve reflects several oscillations through the studied section (**Fig.**  
192 **5**). A positive  $\delta^{13}\text{C}_{\text{bel}}$  shift, showing average values of 1.6‰ is recorded in the Late  
193 Sinemurian Densinodulum to part of the Macdonnelli subchronozones. From the **latest**  
194 Sinemurian Aplanatum Subchronozone (Raricostatum Chronozone) up to the **Early**  
195 Pliensbachian Valdani Subchronozone of the Ibex Chronozone, average  $\delta^{13}\text{C}_{\text{bel}}$  values  
196 are **-0.1‰**, delineating an about 1–1.5‰ relatively well marked negative excursion. In  
197 the **late** Ibex and **in** the Davoei chronozones, the  $\delta^{13}\text{C}_{\text{bel}}$  curve records background  
198 values of about 1‰, with a positive **excursion** at the **latest** Ibex Chronozone and the  
199 **earliest** Davoei Chronozone.

200 **At the Late** Pliensbachian the  $\delta^{13}\text{C}_{\text{bel}}$  values tend to outline a slightly positive excursion,  
201 interrupted by a small negative peak in the **latest** Spinatum Chronozone. The **Early**  
202 Toarcian curve reflects the presence of a positive  $\delta^{13}\text{C}_{\text{bel}}$  trend which develops above  
203 the here represented stratigraphical levels, up to the Middle Toarcian Bifrons  
204 Chronozone (Gómez et al., 2008) **and a negative excursion recorded in bulk carbonates**  
205 **samples.**

### 206 **3.4 Oxygen isotopes**

207 The  $\delta^{18}\text{O}_{\text{bel}}$  values show the presence of several excursions through the **Late**  
208 Sinemurian to the **Early** Toarcian (Fig. 5). In the **Late** Sinemurian to the **earliest**  
209 Pliensbachian interval, an about 1‰ negative excursion, showing values generally  
210 below -1‰ with peak values up to -3‰ has been recorded in Sinemurian samples  
211 located immediately below the stratigraphic column represented in Fig. 5. In most of  
212 the **Early** Pliensbachian Jamesoni and the **earliest part** of the Ibex chronozones,  $\delta^{18}\text{O}_{\text{bel}}$   
213 values are quite stable, around -1‰, but another about 1–1.5‰ negative excursion,  
214 with peak values up to -1.9‰, develops along most of the **Early** Pliensbachian Ibex and  
215 Davoei chronozones, extending up to the base of the **Late** Pliensbachian Margaritatus  
216 Chronozone. Most of the **Late** Pliensbachian and the **earliest** Toarcian are  
217 characterized by the presence of an important change. **An in the order of 1.5‰  $\delta^{18}\text{O}_{\text{bel}}$**   
218 **positive excursion**, with frequent values around 0‰, and positive values up to 0.7‰,  
219 were assayed in this interval. The oxygen isotopes recorded a new change on its  
220 tendency in the **Early** Toarcian, where a prominent  **$\delta^{18}\text{O}_{\text{bel}}$  negative excursion**, about  
221 1.5–2‰ with values up to -3‰, has been verified.

## 222 **4 Discussion**

223 The isotope curves obtained in the Upper Sinemurian, Pliensbachian and Lower  
224 Toarcian section of the Asturian Basin has been correlated with other successions of  
225 similar age, in order to evaluate if the recorded environmental features have a local or  
226 a possible global extent. In order to correlate a more homogeneous dataset, only the  
227 isotopic results obtained by other authors from belemnite calcite and exceptionally  
228 from brachiopod calcite, have been used for the correlation of the stable isotopic data.

### 229 **4.1. Reliability of belemnite isotope records**

230 **Discussion on the palaeoecology of belemnites and the validity of the isotopic data**  
231 **obtained from belemnite calcite for the calculation of palaeotemperatures is beyond**  
232 **the scope of this paper, but the use of belemnite calcite as a proxy is generally**  
233 **accepted and widely used as a reliable tool for palaeothermometry in most of the**  
234 **Mesozoic. However, palaeoecology of belemnites is a source of conflicts** because, as  
235 **extinct organisms, there is a complete lack of understanding of fossil belemnite**  
236 **ecology (Rexfort and Mutterlose, 2009). Belemnite lived as active predators with a**  
237 **swimming life habitats. Nevertheless, several authors (Anderson et al., 1994; Mitchell,**  
238 **2005; Wierzbowski and Joachimiski, 2007) proposed a bottom-dwelling mode of life on**  
239 **the basis of oxygen isotope thermometry, similar to modern sepiids which show a**  
240 **nektobenthic mode of life. This is contradicted by the occurrence of various belemnite**  
241 **genera in black shales that lack any benthic or nektobenthic organisms due to anoxic**  
242 **bottom waters (i.e. the Lower Jurassic Posidonienschiefer, see Rexfort and Mutterlose,**  
243 **2009), indicating that belemnites had a nektonic rather than a nektobenthic mode of**  
244 **life (Mutterlose et al., 2010). As Rexfort and Mutterlose (2009) stated, it is unclear**  
245 **whether isotopic data from belemnites reflect a surface or a deeper water signal and**  
246 **we do not know if the belemnites mode of life changed during ontogeny. Similarly, Li**  
247 **et al. (2012) concluded that belemnites were mobile and experienced a range of**  
248 **environmental conditions during growth and that some belemnite species inhabited**  
249 **environmental niches that remain unchanged, while other species had a more**  
250 **cosmopolitan lifestyle inhabiting wider environments. To complete the scenario,**  
251 **Mutterlose et al. (2010) suggested different lifestyles (nektonic versus nektobenthic) of**

252 belemnites genera as indicated by different shaped guards. Short, thick guards could  
253 indicate nekto-benthic lifestyle, elongated forms fast swimmers, and extremely flattened  
254 guards benthic lifestyle.

255 The Ullmann et al. (2014) work hypothesises that belemnites (*Passaloteuthis*) of the  
256 Lower Toarcian Tenuicostatum Zone had a nekto-benthic lifestyle and once became  
257 extinct (as many organisms in the Early Toarcian mass extinction) were substituted by  
258 belemnites of the genus *Acrocoelites* supposedly of nektonic lifestyle that these  
259 authors impute as due to anoxia.

260 On the other hand, the isotopic studies performed on present-day cuttlefish (*Sepia*  
261 sp.), which are assumed to be the most similar group equivalent to belemnites, reveals  
262 that all the specimens (through their  $\delta^{18}\text{O}$  signal) reflect the temperature-  
263 characteristics of their habitat perfectly (Rexfort and Mutterlose, 2009). Also the  
264 studies of Bettencourt and Guerra (1999), performed in cuttlebone of *Sepia officinalis*  
265 conclude that the obtained  $\delta^{18}\text{O}$  temperature agreed with changes in temperature of  
266 seawater, supporting the use of belemnites as excellent tools for calculation of  
267 palaeotemperatures.

268 It seems that at least some belemnites could swim through the water column,  
269 reflecting the average temperature and not necessarily only the temperature of the  
270 bottom water or of the surface water. In any case, instead of single specific values,  
271 comparisons of average temperatures to define the different episodes of temperature  
272 changes are used in this work.

273

#### 274 4.2. Carbon isotope curve

275 The  $\delta^{13}\text{C}_{\text{bel}}$  carbon isotope excursions (CIEs) found in the Asturian Basin, can be  
276 followed in other sections across Western Europe (Fig. 6). The Late Sinemurian positive  
277 CIE has also been recorded in the Cleveland Basin of the UK by Korte and Hesselbo  
278 (2011) and in the  $\delta^{13}\text{C}_{\text{org}}$  data of the Wessex Basin of southern UK by Jenkyns and  
279 Weedon (2013).

280 The Early Pliensbachian  $\delta^{13}\text{C}_{\text{bel}}$  negative excursion that extends from the Raricostatum  
281 Chronozone of the latest Sinemurian to the Early Pliensbachian Jamesoni and part of  
282 the Ibex chronozones (Fig. 6), correlates with the lower part of the  $\delta^{13}\text{C}_{\text{bel}}$  negative  
283 excursion reported by Armendáriz et al. (2012) in another section of the Asturian  
284 Basin. Similarly, the  $\delta^{13}\text{C}_{\text{bel}}$  curve obtained by Quesada et al. (2005) in the neighbouring  
285 Basque–Cantabrian Basin shows the presence of a negative CIE in similar  
286 stratigraphical position. In the Cleveland Basin of the UK, the studies on the  
287 Sinemurian–Pliensbachian deposits carried out by Hesselbo et al. (2000), Jenkyns et al.  
288 (2002) and Korte and Hesselbo (2011) reflect the presence of this Early Pliensbachian  
289  $\delta^{13}\text{C}_{\text{bel}}$  decrease of values. In the Peniche section of the Lusitanian Basin of Portugal,  
290 this negative CIE has also been recorded by Suan et al. (2010) in brachiopod calcite,  
291 and in bulk carbonates in Italy (Woodfine et al., 2008; Francheschi et al., 2014). The  
292 about 1.5–2‰ magnitude of this negative excursion seems to be quite consistent  
293 across the different European localities.

294 Korte and Hesselbo (2011) pointed out that the Early Pliensbachian  $\delta^{13}\text{C}$  negative  
295 excursion seems to be global in character and the result of the injection of isotopically

296 light carbon from some remote source, such as methane from clathrates, wetlands, or  
297 thermal decomposition or thermal metamorphism or decomposition of older organic-  
298 rich deposits. However none of these possibilities have been documented yet.

299 Higher in the section, the  $\delta^{13}\text{C}$  values are relatively uniform, except for a thin interval,  
300 around the **Early** Pliensbachian IbeX–Davoei zonal boundary, where a small positive  
301 **excursion** (the IbeX–Davoei positive **excursion**, previously mentioned by Rosales et al.,  
302 **2001** and by Jenkyns et al., **2002**) can be observed in most of the  $\delta^{13}\text{C}$  curves  
303 summarized in **Fig. 6, as well as in the carbonates of the Portuguese Lusitanian Basin**  
304 **(Silva et al., 2011).**

305 The next CIE is a **positive excursion** about 1.5–2‰, well recorded in all the correlated  
306 Upper Pliensbachian sections (the **Late** Pliensbachian positive excursion in **Fig. 6**) and  
307 **in bulk carbonates of the Lusitanian Basin (Silva et al., 2011; Silva and Duarte, 2015 and**  
308 **in the Apennines of Central Italy by Moretinni et al., 2002).** This CIE also partly  
309 **coincides with the  $\delta^{13}\text{C}_{\text{org}}$  reported by Caruthers et al. (2014) in Western North**  
310 **America.** Around the Pliensbachian–Toarcian boundary, a negative  $\delta^{13}\text{C}$  peak is again  
311 recorded (**Fig. 6**). This narrow excursion was described by Hesselbo et al. (2007) in bulk  
312 rock samples in Portugal, and tested by Suan et al. (2010) in the same basin and  
313 extended to the Yorkshire (UK) by Littler et al. (2010) and by Korte and Hesselbo  
314 (2011). If this perturbation of the carbon cycle is global, as Korte and Hesselbo (2011)  
315 pointed out, it could correspond with the negative  $\delta^{13}\text{C}$  peak recorded in the upper  
316 part of the Spinatum Chronozone in the Asturian Basin (this work); with the negative  
317  $\delta^{13}\text{C}$  peak reported by Quesada et al. (2005) in the same stratigraphical position in the  
318 Basque–Cantabrian Basin, and **with** the  $\delta^{13}\text{C}$  negative peak reported by van de  
319 Schootbrugge et al. (2010) and Harazim et al. (2013) in the French Grand Causses  
320 Basin.

321 Finally, the **Early** Toarcian is characterized by a prominent  **$\delta^{13}\text{C}$  positive excursion** that  
322 has been detected in all the here considered sections, as well as in some South  
323 American (Al-Suwaidi et al., 2010) and Northern African (Bodin et al., 2010) sections,  
324 **which is interrupted by an about 1‰  $\delta^{13}\text{C}_{\text{bulk}}$  negative excursion located around the**  
325 **Tenuicostatum–Serpentinum zonal boundary.**

326 The origin of the positive excursion has been interpreted by some authors as the  
327 response of water masses to excess and rapid burial of large amounts of organic  
328 carbon rich in  $^{12}\text{C}$ , which led to enrichment in  $^{13}\text{C}$  of the sediments (Jenkyns and  
329 Clayton, 1997; Schouten et al., 2000). Other authors ascribe the origin of this positive  
330 excursion to the removal from the oceans of large amounts of isotopically light carbon  
331 as organic matter into black shales or methane hydrates, resulting from ebullition of  
332 isotopically heavy  $\text{CO}_2$ , generated by methanogenesis of organic-rich sediments  
333 (McArthur et al., 2000).

334 Although  **$\delta^{13}\text{C}$  positive excursions** are difficult to account for (Payne and Kump, 2007),  
335 it seems that this **positive CIE** cannot necessarily be the consequence of the  
336 widespread preservation of organic-rich facies under anoxic waters, as no anoxic facies  
337 are present in the Spanish Lower Toarcian sections (Gómez and Goy, 2011). Modelling  
338 of the CIEs performed by Kump and Arthur (1999) shows that  **$\delta^{13}\text{C}$  positive excursions**  
339 can also be due to an increase in the rate of phosphate or phosphate and inorganic



340 carbon delivery to the ocean, and that large positive excursions in the isotopic  
341 composition of the ocean can also be due to an increase in the proportion of  
342 carbonate weathering relative to organic carbon and silicate weathering. Other  
343 authors argue that increase of  $\delta^{13}\text{C}$  in bulk organic carbon may reflect a massive  
344 expansion of marine archaea bacteria that do not isotopically discriminate in the type  
345 of carbon they use, leading to positive  $\delta^{13}\text{C}$  shifts (Kidder and Worsley, 2010).

346 The origin of the Early Toarcian  $\delta^{13}\text{C}$  negative excursion has been explained by several  
347 papers as due to the massive release of large amounts of isotopically light  $\text{CH}_4$  from  
348 the thermal dissociation of gas hydrates Hesselbo et al. (2000, 2007), Cohen et al.  
349 (2004) and Kemp et al. (2005), with the massive release of gas methane linked with the  
350 intrusion of the Karoo-Ferrar large igneous province onto coalfields, as proposed by  
351 McElwain et al. (2005) or with the contact metamorphism by dykes and sills related to  
352 the Karoo-Ferrar igneous activity into organic-rich sediments (Svensen et al., 2007).

353 Martinez and Dera (2015) proposed the presence of fluctuation in the carbon cycle  
354 during the Jurassic and Early Cretaceous, due to a cyclicity of  $\sim 9$  My linked to a great  
355 eccentricity cycle, amplified by cumulative sequestration of organic matter.  
356 Nevertheless, this  $\sim 9$  My cycle has not been evidenced in the Pliensbachian deposits of  
357 several parts of the World (Ikeda and Tada, 2013, 2014) and cannot be evidenced in  
358 the Pliensbachian deposits of the Asturian Basin. The disruption of this cyclicity  
359 recorded during the Pliensbachian could be linked to chaotic behaviour in the solar  
360 system (Martinez and Dera, 2015) possibly due to the chaotic transition in the  
361 Earth–Mars resonance (Ikeda and Tada, 2013). Data from Japan suggests that this  
362 disruption developed from the Hettangian to the Pliensbachian (Ikeda and Tada, 2013,  
363 2014) was possibly linked to the massive injection of  $\text{CO}_2$  from the eruptions of the  
364 Central Atlantic Magmatic Province to the Karoo-Ferrar eruptions (Prokoph et al. 2013)  
365 which destabilized the carbon fluxes, reducing or dephasing the orbital imprint in the  
366  $\delta^{13}\text{C}$  over millions of years (Martinez and Dera, 2015).

#### 367 **4.3. Oxygen isotope curves and seawater palaeotemperature oscillations**

368 Seawater palaeotemperature calculation from the obtained  $\delta^{18}\text{O}$  values reveals the  
369 occurrence of several isotopic events corresponding with relevant climatic oscillations  
370 across the latest Sinemurian, the Pliensbachian and the Early Toarcian (Fig. 7). Some of  
371 these climatic changes could be of global extent. In terms of seawater  
372 palaeotemperature, five intervals can be distinguished. The earliest interval  
373 corresponds with a warming period developed during the Late Sinemurian up to the  
374 earliest Pliensbachian. Most of the Early Pliensbachian is represented by a period of  
375 “normal” temperature, close to the average palaeotemperatures of the studied  
376 interval. A new warming period is recorded at the Early–Late Pliensbachian transition,  
377 and the Late Pliensbachian is represented by an important cooling interval. Finally the  
378 Early Toarcian coincides with a severe (super)warming interval, linked to the important  
379 Early Toarcian mass extinction (Gómez and Arias, 2010; García Joral et al., 2011;  
380 Gómez and Goy, 2011; Fraguas et al., 2012; Clémence, 2014; Clémence et al., 2015;  
381 Baeza-Carratalá et al., 2015). The average palaeotemperature of the latest Sinemurian,  
382 Pliensbachian (palaeolatitude of  $32^\circ\text{N}$ ) and Early Toarcian (palaeolatitude of  $40^\circ\text{N}$ ),  
383 calculated from the  $\delta^{18}\text{O}$  values obtained from belemnite calcite in this work, is  $15.6^\circ\text{C}$ .

#### 384 4.3.1. The Late Sinemurian Warming

385 The **earliest** isotopic event is a  $\delta^{18}\text{O}$  **negative excursion** that develops in the **Late**  
386 Sinemurian Raricostatum Chronozone, up to the **earliest** Pliensbachian Jamesoni  
387 Chronozone. Average palaeotemperatures calculated from the  $\delta^{18}\text{O}$  belemnite samples  
388 collected below the part of the **Late** Sinemurian Raricostatum Chronozone represented  
389 in **figure 5** were 19.6°C. This temperature increases to 21.5°C in the lower part of the  
390 Raricostatum Chronozone (Densinodulum Subchronozone), and temperature  
391 progressively decreases through the **latest** Sinemurian and **earliest** Pliensbachian. In  
392 the **Raricostatum** Subchronozone, the average calculated temperature is 18.7°C; in the  
393 Macdonnelli Subchronozone average temperature is 17.5°C and average values of  
394 16.7°C, closer to the average temperatures **of the studied interval**, are not reached  
395 until the **latest** Sinemurian Aplanatum Subchronozone and the **earliest** Pliensbachian  
396 Taylori–Polymorphus subchronozones. All these values delineate a warming interval  
397 mainly developed in the **Late** Sinemurian (**Figs. 7, 8**) **on which the general trend is a**  
398 **decrease in palaeotemperature from the Late Sinemurian to the earliest Pliensbachian.**

399 The **Late** Sinemurian Warming interval is also recorded in the Cleveland Basin of the UK  
400 (Hesselbo et al., 2000; Korte and Hesselbo, 2011). The belemnite-based  $\delta^{18}\text{O}$  values  
401 obtained by these authors are in the order of  $-1\text{‰}$  to  $-3\text{‰}$ , with peak values lower  
402 than  $-4\text{‰}$ . That represents a range of palaeotemperatures normally between 16 and  
403 24°C with peak values up to 29°C, which are not compatible with a cooling, but with a  
404 warming interval.

405 The **Late** Sinemurian warming coincides only partly with the **Early** Pliensbachian  $\delta^{13}\text{C}$   
406 **negative excursion**, located near the stage boundary (**Fig. 6**). Consequently, this **warm**  
407 cannot be fully interpreted as the consequence of the release of methane from  
408 clathrates, wetlands or decomposition of older organic-rich sediments, as interpreted  
409 by Korte and Hesselbo (2011) because only a small portion of both excursions are  
410 coincident.

#### 411 4.3.2. The “normal” temperature **Early Pliensbachian Jamesoni Chronozone interval**

412 After the Late Sinemurian Warming,  $\delta^{18}\text{O}$  values are around  $-1\text{‰}$  reflecting average  
413 palaeotemperatures of about 16°C (**Fig. 7**). This Early Pliensbachian interval of  
414 “normal” (**average**) temperature develops in most of the Jamesoni Chronozone and  
415 the base of the Ibex Chronozone (**Fig. 8**). In the Taylori–Polymorphus chronozones,  
416 average temperature is 15.7°C, in the Brevispina Subchronozone is 16.4°C, and in the  
417 Jamesoni Subchronozone 17.2°C. Despite showing more variable data, this interval has  
418 also been recorded in other sections of the Asturian Basin (**Fig. 8**) by Armendáriz et al.  
419 (2012), and relatively uniform values are also recorded in the Basque–Cantabrian Basin  
420 of Northern Spain (Rosales et al., 2004) and in the Peniche section of the Portuguese  
421 Lusitanian Basin (Suan et al., 2008, 2010). Belemnite calcite-based  $\delta^{18}\text{O}$  values  
422 published by Korte and Hesselbo (2011) are quite **scattered**, oscillating between  $\sim 1\text{‰}$   
423 and  $\sim -4.5\text{‰}$  (**Fig. 8**).

#### 424 4.3.3. The Early Pliensbachian Warming interval

425 Most of the Early Pliensbachian Ibex Chronozone and the base of the **Late**  
426 Pliensbachian are dominated by a 1 to 1.5%  $\delta^{18}\text{O}$  **negative excursion**, representing an

427 increase in palaeotemperature, which marks a new warming interval. Average values  
428 of 18.2°C with peak values of 19.7°C were reached in the Rodiles section (Fig. 7). This  
429 increase in temperature partly co-occurs with the latest part of the Early Pliensbachian  
430  $\delta^{13}\text{C}$  negative excursion.

431 The Early Pliensbachian Warming interval is also well marked in other sections of  
432 Northern Spain (Fig. 8) like in the Asturian Basin (Armendáriz et al., 2012) and the  
433 Basque–Cantabrian Basin (Rosales et al., 2004), where peak values around 25°C were  
434 reached. The increase in seawater temperature is also registered in the Southern  
435 France Grand Causses Basin (van de Schootbrugge et al., 2010), where temperatures  
436 averaging around 18°C have been calculated. This warming interval is not so clearly  
437 marked in the brachiopod calcite of the Peniche section in Portugal (Suan et al., 2008,  
438 2010), but even very scattered  $\delta^{18}\text{O}$  values, peak palaeotemperature near 30°C were  
439 frequently reported in the Cleveland Basin (Korte and Hesselbo, 2011). In the  
440 compilation performed by Dera et al. (2009, 2011) and Martínez and Dera (2015),  $\delta^{18}\text{O}$   
441 values are quite scattered, but this Early Pliensbachian Warming interval is also well  
442 marked. Data on neodymium isotope presented by Dera et al. (2009) indicate the  
443 presence of a generalized southwards directed current in the Euro-boreal waters for  
444 most of the Early Jurassic, except for the Early–Late Pliensbachian transition, where a  
445 positive  $\epsilon_{\text{Nd}}$  excursion suggests northward influx of warmer Tethyan or Panthalassan  
446 waters which could contribute to the seawater warming detected in the Early  
447 Pliensbachian.

#### 448 4.3.4. The Late Pliensbachian Cooling interval

449 One of the most important Jurassic  $\delta^{18}\text{O}$  positive excursions is recorded by belemnites  
450 from the Late Pliensbachian to the Early Toarcian in all the correlated localities (Figs. 5,  
451 7, 8). This represents an important climate change towards cooler temperatures that  
452 begins at the base of the Late Pliensbachian and extends up to the earliest Toarcian  
453 Tenuicostatum Chronozone, representing an about 4 Myrs major cooling interval.  
454 Average palaeotemperatures of 12.7°C for this period in the Rodiles section have been  
455 calculated by supposing the absence of ice caps, and peak temperatures as low as  
456 9.5°C were recorded in several samples from the Gibbosus and the Apyrenum  
457 subchronozones (Fig. 7).

458 This major cooling event has been recorded in many parts of the World. In Europe, the  
459 onset and the end of the cooling interval seems to be synchronous at the scale of  
460 ammonites subchronozones (Fig. 8). It starts at the Stokesi Subchronozones of the  
461 Margaritatus Chronozone (near the onset of the Late Pliensbachian), and extends up to  
462 the Early Toarcian Semicelatum Subchronozones of the Tenuicostatum Chronozone. In  
463 addition to the Asturian Basin (Gómez et al., 2008; Gómez and Goy, 2011; this work), it  
464 has clearly been recorded in the Basque–Cantabrian Basin (Rosales et al., 2004; Gómez  
465 and Goy, 2011; García Joral et al., 2011) and in the Iberian Basin of Central Spain  
466 (Gómez et al., 2008; Gómez and Arias, 2010; Gómez and Goy, 2011), in the Cleveland  
467 Basin of the UK (McArthur et al., 2000; Korte and Hesselbo, 2011), in the Lusitanian  
468 Basin (Suan et al., 2008, 2010), in the French Grand Causses Basin (van de  
469 Schootbrugge et al., 2010), and in the data compiled by Dera et al. (2009, 2011).

470 As for many of the major cooling periods recorded in the Phanerozoic, low levels of  
471 atmospheric  $p\text{CO}_2$ , and/or variations in oceanic currents related to the break-up of  
472 Pangea could explain these changes in seawater (Dera et al., 2009; 2011). The  
473 presence of relatively low  $p\text{CO}_2$  levels in the Late Pliensbachian atmosphere is  
474 supported by the value of  $\sim 900$  ppm obtained from Pliensbachian araucariacean leaf  
475 fossils of southeastern Australia (Steinthorsdottir and Vajda, 2015). These values are  
476 much higher than the measured Quaternary preindustrial 280 ppm  $\text{CO}_2$  (i.e. Wigley et  
477 al., 1996), but lower than the  $\sim 1000$  ppm average estimated for the Early Jurassic. The  
478 recorded Pliensbachian values represent the minimum values of the Jurassic and of  
479 most of the Mesozoic, as documented by the GEOCARB II (Berner, 1994), and the  
480 GEOCARB III (Berner and Kothavala, 2001) curves, confirmed for the Early Jurassic by  
481 Steinthorsdottir and Vajda (2015). Causes of this lowering of atmospheric  $p\text{CO}_2$  are  
482 unknown but they could be favoured by elevated silicate weathering rates, nutrient  
483 influx, high primary productivity, and organic matter burial (Suan et al., 2010; Silva and  
484 Duarte, 2015).

485 It seems that the **Late** Pliensbachian represents a time interval of major cooling,  
486 probably of global extent. This fact has conditioned that many authors point to this  
487 period as one of the main candidates for the development of polar ice caps in the  
488 Mesozoic (Price, 1999; Guex et al., 2001; Dera et al., 2011; Suan et al., 2011; Gómez  
489 and Goy, 2011; Fraguas et al., 2012). This idea is based on the presence, in the Upper  
490 Pliensbachian deposits of different parts of the World, of: 1) glendonites; 2) exotic  
491 pebble to boulder-size clasts; 3) the presence in some localities of a hiatus in the Late  
492 Pliensbachian–earliest Toarcian; 4) the results obtained in the General Circulation  
493 Models, and 5) the calculated Late Pliensbachian palaeotemperatures and the  
494 assumed pole-to-equator temperature gradient.

#### 495 **4.3.4. The **Early** Toarcian Superwarming interval**

496 Seawater temperature started to increase at the **earliest** Toarcian. From an average  
497 temperature of  $12.7^\circ\text{C}$  during the **Late** Pliensbachian Cooling interval, average  
498 temperature rose to  $15^\circ\text{C}$  in the upper part of the **earliest** Toarcian Tenuicostatum  
499 Chronozone (Semicelatum Subchronozone), which represents a progressive increase  
500 on seawater temperature in the order of  $2\text{--}3^\circ\text{C}$ . **Atmospheric  $\text{CO}_2$  concentration during  
501 the Early Toarcian seems to be doubled from  $\sim 1000$  ppm to  $\sim 2000$  ppm (i.e. Berner,  
502 2006; Retallack, 2009; Steinthorsdottir and Vajda, 2015), causing this important and  
503 rapid warming. Comparison** of the evolution of palaeotemperature with the evolution  
504 of the number of taxa reveals that progressive warming coincides first with a  
505 progressive loss in the taxa of several groups (Gómez and Arias, 2010; Gómez and Goy,  
506 2011; García Joral et al., 2011; Fraguas et al., 2012; Baeza-Carratalá et al., 2015)  
507 marking the prominent **Early** Toarcian extinction interval. Seawater palaeotemperature  
508 rapidly increased around the Tenuicostatum–Serpentinum zonal boundary, where  
509 average values of about  $21^\circ\text{C}$ , with peak temperatures of  $24^\circ\text{C}$  were reached (Fig. 7).  
510 This important warming, which represents a  $\Delta T$  of about  $8^\circ\text{C}$  respect to the average  
511 temperatures of the **Late** Pliensbachian Cooling interval, coincides with the turnover of  
512 numerous groups (Gómez and Goy, 2011) the total disappearance of the brachiopods  
513 (García Joral et al., 2011; Baeza-Carratalá et al., 2015), the extinction of numerous  
514 species of ostracods (Gómez and Arias, 2010), and a crisis of the nannoplankton

515 (Fraguas, 2010; Fraguas et al., 2012; Clémence et al., 2015). Temperatures remain high  
516 and relatively constant through the Serpentinum and Bifrons chronozones, and the  
517 platforms were repopulated by opportunistic immigrant species that thrived in the  
518 warmer Mediterranean waters (Gómez and Goy, 2011).

## 519 **5. Conclusions**

520 Several relevant climatic oscillations across the **Late** Sinemurian, the Pliensbachian and  
521 the **Early** Toarcian have been documented in the Asturian Basin. Correlation of these  
522 climatic changes with other European records points out that some of them could be  
523 of global extent. In the **Late** Sinemurian, a warm interval showing average temperature  
524 of 18.5°C was recorded. The end of this warming interval coincides with the onset of a  
525  $\delta^{13}\text{C}$  negative excursion that develops through the **latest** Sinemurian and part of the  
526 **Early** Pliensbachian.

527 The **Late** Sinemurian **Warming** interval is followed by an interval of “normal”  
528 temperature averaging 16°C, which develops through most of the **Early** Pliensbachian  
529 Jamesoni Chronozone and the base of the Ibex Chronozone.

530 The **latest** part of the **Early** Pliensbachian is dominated by an increase in temperature,  
531 marking **another** warming interval which extends to the base of the **Late** Pliensbachian,  
532 where average temperature of 18.2 °C was calculated. Within this warming interval, a  
533  $\delta^{13}\text{C}$  positive peak occurs at the transition between the **Early** Pliensbachian Ibex and  
534 Davoei chronozones.

535 One of the most important climatic changes was recorded through the **Late**  
536 Pliensbachian. Average palaeotemperature of 12.7°C for this interval in the Rodiles  
537 section delineated an about 4 Myrs major **Late** Pliensbachian Cooling event that was  
538 recorded in many parts of the World. At least in Europe, the onset and the end of this  
539 cooling interval is synchronous at the scale of ammonites subchronozone. The cooling  
540 interval coincides with a  $\delta^{13}\text{C}$  slightly positive excursion, interrupted by a small  
541 negative  $\delta^{13}\text{C}$  peak in the **latest** Pliensbachian Hawskerense Chronozone. This  
542 prominent cooling event has been pointed as one of the main candidates for the  
543 development of polar ice caps in the Jurassic.

544 Seawater temperature started to increase at the **earliest** Toarcian, rising to 15°C in the  
545 **latest** Tenuicostatum Chronozone (Semicelatum Subchronozone), and seawater  
546 palaeotemperature considerably increased around the Tenuicostatum–Serpentinum  
547 zonal boundary, reaching average values in the order of 21°C, with peak intervals of  
548 24°C, which coincides with the Early Toarcian major extinction event, pointing  
549 warming as the main cause of the faunal turnover.

550

## 551 Acknowledgments

552 **Prof. Appy Sluijs and three anonymous reviewers are thanked for their comments and**  
553 **suggestions that improved the manuscript.** This research work was financed by  
554 projects CGL 2011–25894 and CGL2011-23947 (MICINN) of the Spanish Ministerio de  
555 Economía y Competitividad, and by projects GR3/14/910431, and GI 910429 of the

556 Universidad Complutense de Madrid. Thanks to the Instituto Geológico y Minero de  
557 España for allowing the use of the cathodoluminescence microscope.

558

## 559 **References**

560 Al-Suwaidi, A.H., Angelozzi, G.N., Baudin, F., Damborenea, S.E., Hesselbo, S.P., Jenkyns,  
561 H.C., Manceñido, M.O. and Riccardi, A.C.: First record of the Early Toarcian  
562 Oceanic Anoxic Event from the Southern Hemisphere, Neuquén Basin,  
563 Argentina, *J. Geol. Soc. London*, 167, 633–636, 2010.

564 Anderson, T.F. and Arthur, M.A.: Stable isotopes of oxygen and carbon and their  
565 application to sedimentologic and paleoenvironmental problems, in: *Stable*  
566 *isotopes in sedimentary geology*, edited by Arthur, M.A., SEPM Short Course  
567 10, 1-1-1-151, 1983.

568 **Anderson, T.F., Popp, B.N., Williams, A.C., Ho, L.Z. and Hudson, J.D.: The stable isotopic**  
569 **record of fossils from the Peterborough Member, Oxford Clay Formation**  
570 **(Jurassic), UK: palaeoenvironmental implications. *J. Geol. Soc. London*, 151.**  
571 **125–138, 1994.**

572 Armendáriz, M., Rosales, I., Bádenas, B., Aurell, M., García-Ramos, J.C. and Piñuela, L.:  
573 High-resolution chemostratigraphic record from Lower Pliensbachian  
574 belemnites: Palaeoclimatic perturbations, organic facies and water mass  
575 Exchange (Asturian basin, northern Spain), *Palaeogeogr. Palaeocl.*, 333–334,  
576 178–191, 2012.

577 Bádenas, B, Aurell, M., García-Ramos, J.C., González, B. and Piñuela, L.: Sedimentary vs.  
578 Diagenetic control on rhythmic calcareous successions (Pliensbachian of Asturias,  
579 Spain), *Terra Nova*, 21, 162–170, 2009.

580 Bádenas, B, Aurell, M., Armendáriz, M., Rosales, I., García-Ramos, J.C. and Piñuela, L.:  
581 Sedimentary and chemostratigraphic record of climatic cycles in Lower  
582 Pliensbachian marl–limestone platform successions of Asturias (North Spain),  
583 *Sed. Geol.*, 281, 119–138, 2012.

584 Baeza-Carratalá, J.F., García Joral, F., Giannetti, A. and Tent-Manclús, J.E.: Evolution of  
585 the last koninckinids (Athyrida, Koninckidae), a precursor signal of the early  
586 Toarcian mass extinction event in the Western Tethys, *Palaeogeogr. Palaeocl.*,  
587 429, 41–56, 2015.

588 Bailey, T.R., Rosenthal, Y., McArthur, J.M., van de Schootbrugge, B. and Thirlwall, M.F.:  
589 Paleooceanographic changes of the Late Pliensbachian–Early Toarcian interval: a  
590 possible link to the genesis of an Oceanic Anoxic event, *Earth Planet. Sc. Lett.*,  
591 212, 307–320, 2003.

592 Benito, M.I. and Reolid, M.: Belemnite taphonomy (Upper Jurassic, Western Tethys)  
593 part II: Fossil–diagenetic analysis including combined petrographic and  
594 geochemical techniques, *Palaeogeogr. Palaeocl.*, 358–360, 89–108, 2012.

- 595 Berner, R.A.: GEOCARB II: A revised model of atmospheric CO<sub>2</sub> over Phanerozoic time.  
596 Am. J. Sci. 249, 56–41, 1994. A revised model of atmospheric CO<sub>2</sub> over  
597 Phanerozoic time, Am. J. Sci., 249, 56–41, 1994.
- 598 Berner, R.A.: GEOCARBSUL: a combined model for Phanerozoic atmospheric O<sub>2</sub> and  
599 CO<sub>2</sub>, Geochim. Cosmochim. Ac., 70, 5653–5664, 2006.
- 600 Berner, R.A. and Kothavala, Z. GEOCARB III. A revised model of atmospheric CO<sub>2</sub> over  
601 Phanerozoic time, Am. J. Sci., 301, 182–204, 2001.
- 602 Bettencourt, V. and Guerra, A.: Carbon- and Oxygen-isotope composition of the  
603 cuttlebone of *Sepia officinalis*: a tool for predicting ecological information, Mar.  
604 Biol., 133, 651–657, 1999.
- 605 Bodin, S., Mattioli, E., Fröhlich, S., Marshall, J.D., Boutib, L., Lahsini, S. and Redfern, J.:  
606 Toarcian carbon isotope shifts and nutrient changes from the Northern margin  
607 of Gondwana (High Atlas, Morocco, Jurassic): Palaeoenvironmental  
608 implications, Palaeogeogr. Palaeocl., 297, 377–390, 2010.
- 609 Caruthers, A.W., Smith, P.L., Gröcke, D.R.: The Pliensbachian–Toarcian (Early Jurassic)  
610 extinction: A North American perspective. in: *Volcanism, Impacts and Mass*  
611 *Extinctions: Causes and Effects*, edited by Keller, G. and Kerr, A.C., Geo. Soc. Am.  
612 Spec. Paper 505, 225–243, 2014.
- 613 Chandler, M.A., Rind, D. and Ruedy, R.: Pangaeian climate during the Early Jurassic:  
614 GCM simulations and the sedimentary record of paleoclimate, Geol. Soc. Am.  
615 Bull., 104, 543–559, 1992.
- 616 Clémence, M.E.: Pattern and timing of the Early Jurassic calcareous nannofossil crisis,  
617 Palaeogeogr. Palaeocl., 411, 56–64, 2014.
- 618 Clémence, M.E., Gardin, S. and Bartolini A.: New insights in the pattern and timing of  
619 the Early Jurassic calcareous nannofossil crisis, Palaeogeogr. Palaeocl., 427,  
620 100–108, 2015.
- 621 Cohen, A.S., Coe, A.L., Harding, S.M. and Schwark, L.: Osmium isotope evidence for  
622 regulation of atmospheric CO<sub>2</sub> by continental weathering. *Geology*, 32,  
623 157–160, 2004
- 624 Comas-Rengifo, M.J. and Goy, A.: Caracterización biocronoestratigráfica del  
625 Sinemuriense Superior y el Pliensbachense entre los afloramientos de Playa de  
626 Vega y de Lastres (Asturias), in: *Las sucesiones margo-calcáreas marinas del*  
627 *Jurásico Inferior y las series fluviales del Jurásico Superior. Acantilados de Playa*  
628 *de Vega (Ribadesella)*, edited by: García-Ramos J.C. (Coord.), V Congreso  
629 *Jurásico de España*, MUJA, 9–18, 2010.
- 630 Dera, G., Pucéat, E., Pellenard, P., Neige, P., Delsate, D., Joachimski, M.M., Reisberg, L.  
631 and Martinez, M.: Water mass exchange and variations in seawater  
632 temperature in the NW Tethys during the Early Jurassic: Evidence from  
633 neodymium and oxygen isotopes of fish teeth and belemnites, *Earth. Planet. Sc.*  
634 *Lett.*, 286, 198–207, 2009.

- 635 Dera, G., Neige, P., Dommergues, J.L., Fara, E., Lafont, R. and Pellenard, P.: High-  
636 resolution dynamics of Early Jurassic marine extinctions: the case of  
637 Pliensbachian–Toarcian ammonites (Cephalopoda), *J. Geol. Soc. London*, 167,  
638 21–33, 2010.
- 639 Dera, G., Brigaud, B., Monna, F., Laffont, R., Pucéat, E., Deconinck, J.F., Pellenard, P.,  
640 Joachimski, M.M. and Durlet, C.: Climatic ups and downs in a disturbed Jurassic  
641 world, *Geology*, 39, 215–218, 2011.
- 642 Elmi, S., Rulleau, L., Gabilli, J. and Mouterde, R.: Toarcien. Biostratigraphie Jurassique  
643 ouest-européen méditerranéen: zonations parallèles et distribution des  
644 invertébrés et microfossils, edited by Cariou, E. and Hantzpergue, P., *Bull.*  
645 *Centre Rech. Elf Explor. Prod.*, Pau, 17, 25–36, 1997.
- 646 Fraguas, A.: Late Sinemurian–Early Toarcian calcareous nannofossils from the  
647 Cantabrian Basin: spatial and temporal distribution, PhD thesis, *Fac. Sci. Geol.*  
648 *Univ. Complutense Madrid*, Spain, 2010.
- 649 Fraguas, A., Comas-Rengifo, M.J., Gómez, J.J. and Goy, A.: The calcareous nannofossil  
650 crisis in Northern Spain (Asturias province) linked to the Early Toarcian  
651 warming-driven mass extinction, *Mar. Micropaleontol.*, 94–95, 58–71, 2012.
- 652 Frakes, L.A., Francis, J.E. and Syktus, J.I.: *Climate models of the Phanerozoic*, Cambridge  
653 *University Press*. Cambridge, 274 pp, 1992.
- 654 Francheschi, M., Dal Corso, J., Posenato, R., Roghi, Masetti, D. and Jenkyns, H.C.: Early  
655 Pliensbachian (Early Jurassic) C-isotope perturbation and the diffusion of the  
656 Lithiotis Fauna: Insights from the western Tethys, *Palaeogeogr. Palaeoclimatol.*, 410,  
657 255–263, 2014.
- 658 García Joral, F., Gómez, J.J. and Goy, A.: Mass extinction and recovery of the Early  
659 Toarcian (Early Jurassic) brachiopods linked to climate change in northern and  
660 central Spain, *Palaeogeogr. Palaeoclimatol.*, 302, 367–380, 2011.
- 661 Gómez, J.J. and Arias, C.: Rapid warming and ostracods mass extinction at the Lower  
662 Toarcian (Jurassic) of central Spain, *Mar. Micropaleontol.*, 74, 119–135, 2010.
- 663 Gómez, J.J. and Goy, A.: Warming-driven mass extinction in the Early Toarcian (Early  
664 Jurassic) of northern Spain. Correlation with other time-equivalent European  
665 sections, *Palaeogeogr. Palaeoclimatol.*, 306, 176–195, 2011.
- 666 Gómez, J.J., Goy, A. and Canales, M.L.: Seawater temperature and carbon isotope  
667 variations in belemnites linked to mass extinction during the Toarcian (Early  
668 Jurassic) in Central and Northern Spain. Comparison with other European  
669 sections, *Palaeogeogr. Palaeoclimatol.*, 258, 28–58, 2008.
- 670 Goy, A., Comas-Rengifo, M.J., García-Ramos, J.C., Gómez, J.J., Herrero, C., Suárez-Vega,  
671 L.C. and Ureta, M.: The Toarcian Stage in Asturias (North Spain): Ammonites  
672 record, stratigraphy and correlations, *Earth Sci. Frontiers, Spec. Publ.*, 17,  
673 38–39, 2010a.



- 674 Goy, A., Comas-Rengifo, M.J., Gómez, J.J., Herrero, C., Suárez-Vega, L.C. and Ureta, M.:  
675 Biohorizontes de ammonioideos del Toarciense en Asturias, edited by Ruiz  
676 Omeñaca, J.J., Piñuelas, L. and García-Ramos J.C., Com. V Congreso Jurásico de  
677 España, MUJA, 94–102, 2010b.
- 678 Guex, J., Morard, A., Bartolini, A. and Morettini, E.: Découverte d'une importante  
679 lacune stratigraphique à la limite Domérien-Toarcien: implications paléo-  
680 océanographiques, Bull. Soc. Vaud. Sc. Nat., 87, 277–284, 2001.
- 681 Hallam, A.: Jurassic environments, Cambridge Earth Sci. Ser., Cambridge University  
682 Press, Cambridge, 269 pp. 1975.
- 683 Hallam, A.: Jurassic climates as inferred from the sedimentary and fossil record, Philos.  
684 T. R. Soc. B, 342, 287–296, 1993.
- 685 Harazim, D., van de Schootbrugge, B., Sorichter, K., Fiebig, J., Weug, A., Suan, G. and  
686 Oschmann, W.: Spatial variability of watermass conditions within the European  
687 Epicontinental Seaway during the Early Jurassic (Pliensbachian–Toarcian),  
688 Sedimentology, 60, 359–390, 2013.
- 689 Hesselbo, S.P., Gröcke, D.R., Jenkyns, H.C., Bjerrum, C.J., Farrimond, P., Morgans Bell,  
690 H.S. and Green, O.R.: Massive dissociation of gas hydrate during a Jurassic  
691 oceanic anoxic event. *Nature*, 406, 392–395, 2000.
- 692 Hesselbo, S.P., Meister, C. and Gröcke, D.R.: A potential global stratotype for the  
693 Sinemurian–Pliensbachian-boundary (Lower Jurassic), Robin Hood's Bay, UK;  
694 ammonite faunas and isotope stratigraphy, *Geol. Mag.*, 137, 601–607, 2000.
- 695 Hesselbo, S.P., Jenkyns, H.C., Duarte, L.V. and Oliveira, L.C.V.: Carbon-isotope record of  
696 the Early Jurassic (Toarcian) Oceanic Anoxic Event from fossil wood and marine  
697 carbonate (Lusitanian Basin, Portugal), *Earth Planet. Sc. Lett.*, 253, 455–470,  
698 2007.
- 699 Ikeda, M. and Tada, R.: Long period astronomical cycles from the Triassic to Jurassic  
700 bedded chert sequence (Inuyama, Japan): Geologic evidences for the chaotic  
701 behaviour of solar planets. *Earth Planets Space*, 65(4), 351–360, 2013,
- 702 Ikeda, M. and Tada, R.: A 70 million year astronomical time scale for the deep-sea  
703 bedded chert sequence (Inuyama, Japan): Implications for Triassic–Jurassic  
704 geochronology. *Earth. Planet. Sc. Lett.*, 399, 30–43, 2014.
- 705 Jenkyns, H.C.: Evidence for rapid climate change in the Mesozoic-Palaeogene  
706 greenhouse world, *Philos. T. R. Soc. A*, 361, 1885–1916, 2003.
- 707 Jenkyns, H.C. and Clayton, C.J.: Lower Jurassic epicontinental carbonates and  
708 mudstones from England and Wales: chemostratigraphic signals and the early  
709 Toarcian anoxic event, *Sedimentology*, 44, 687–706, 1997.
- 710 Jenkyns, H.C., Jones, C.E., Gröcke, D.R., Hesselbo, S.P. and Parkinson, D.N.:  
711 Chemostratigraphy of the Jurassic System: application, limitations and  
712 implications for palaeoceanography, *J. Geol. Soc. London*, 159, 351–378, 2002.

- 713 Jenkyns, H.C. and Weedon, G.P.: Chemostratigraphy ( $\text{CaCO}_3$ , TOC,  $\delta^{13}\text{C}_{\text{org}}$ ) of  
714 Sinemurian (Lower Jurassic) black shales from the Wessex Basin, Dorset and  
715 palaeoenvironmental implications, *Newsl. on Stratigr.*, 46, 1–21, 2013.
- 716 Kemp, D.B., Coe, A.L., Cohen, A.S. and Schwark, L.: Astronomical pacing of methane  
717 release in the Early Jurassic period, *Nature* 437, 396–399, 2005.
- 718 Kidder, D.L. and Worsley, T.R., Phanerozoic Large Igneous Province (LIPs): HEATT  
719 (Haline Euxinic Acidic Thermal Transgression) episodes, and mass extinctions,  
720 *Palaeogeogr. Palaeoclimatol.*, 295, 162–191, 2010.
- 721 Korte, C. and Hesselbo, S.P.: Shallow marine carbon and oxygen isotope and elemental  
722 records indicate icehouse–greenhouse cycles during the Early Jurassic,  
723 *Paleoceanography*, 26, PA 4219, doi: 10.1029/2011PA002160, 2011.
- 724 Kump, L.R. and Arthur, M.A.: Interpreting carbon-isotope excursions: carbonates and  
725 organic matter, *Chem. Geol.*, 161, 181–198, 1999.
- 726 Li, Q., McArthur, J.M., and Atkinson, T.C.: Lower Jurassic belemnites as indicators of  
727 palaeo-temperature, *Palaeoclimatol. Palaeoecol.*, 315–316, 38–45, 2012.
- 728 Littler, K., Hesselbo, S.P. and Jenkyns, H.C.: A carbon-isotope perturbation at the  
729 Pliensbachian–Toarcian boundary: evidence from the Lias Group, NE England,  
730 *Geol. Mag.*, 147, 181–192, 2010.
- 731 [Martinez, M. And Dera, G.: Orbital pacing of carbon fluxes by a ~9-My eccentricity  
732 cycle during the Mesozoic. \*P. Nat. Acad. Sci. USA\*, 112, 12604–12609, 2015.](#)
- 733 McArthur, J.M., Donovan, D.T., Thirlwall, M.F., Fouke, B.W. and Matthey, D.: Strontium  
734 isotope profile of the early Toarcian (Jurassic) oceanic anoxic event, the  
735 duration of ammonite biozones, and belemnite palaeotemperatures, *Earth  
736 Planet. Sc. Lett.*, 179, 269–285, 2000.
- 737 McArthur, J.M., Doyle, P., Leng, M.J., Reeves, K., Williams, T., García-Sánchez, R. and  
738 Howart, R.J.: Testing palaeo-environmental proxies in Jurassic belemnites:  
739 Mg/Ca, Sr/Ca, Na/Ca,  $\delta^{18}\text{O}$  and  $\delta^{13}\text{C}$ , *Palaeogeogr. Palaeoclimatol.*, 252, 464–480,  
740 2007.
- 741 [McElwain, J.C., Wade-Murphy, J. and Hesselbo, S.P.: Changes in carbon dioxide during  
742 an oceanic anoxic event linked to intrusion into Gondwana coals. \*Nature\*, 435,  
743 479–482, 2005.](#)
- 744 Metodiev, L. and Koleva-Rekalova, E.: Stable isotope records ( $\delta^{18}\text{O}$  and  $\delta^{13}\text{C}$ ) of Lower-  
745 Middle Jurassic belemnites from the Western Balkan mountains (Bulgaria):  
746 Palaeoenvironmental application, *Appl. Geochem.*, 23, 2845–2856, 2008.
- 747 [Mitchel, S.F.: Eight belemnite biohorizons in the Cenomanian of northwest Europe  
748 and their importance. \*Geol. J.\*, 40, 363–382, 2005.](#)
- 749 [Morettini, E., Santantonio, M.; Bartolini, A., Cecca, F., Baumgartner, P.O. and Hunziker, J.C.:  
750 Carbon isotope stratigraphy and carbonate production during the Early–Middle](#)

- 751 [Jurassic: examples from the Umbria–Marche–Sabina Apennines \(central Italy\).](#)  
752 [Palaeogeogr. Palaeocl., 184, 251–273, 2002.](#)
- 753 [Mutterlose, J., Malkoc, M., Schouten, S., Sinninghe Damsté, J.S. and Foster, A.: TEX<sub>86</sub>](#)  
754 [and stable  \$\delta^{18}\text{O}\$  paleothermometry of early Cretaceous sediments: Implications](#)  
755 [for belemnite ecology and palaeotemperature proxy application. Earth Planet.](#)  
756 [Sc. Lett., 298, 286–298, 2010.](#)
- 757 Nikitenko, B.L.: The Early Jurassic to Aalenian paleobiogeography of the arctic realm:  
758 Implication of microbenthos (foraminifers and ostracodes), *Stratigr. Geol.*  
759 *Correl.*, 16, 59–80, 2008.
- 760 Osete, M.L., Gómez, J.J., Pavón-Carrasco, F.J., Villalaín, J.J., Palencia, A., Ruiz-Martínez,  
761 V.C. and Heller, F.: The evolution of Iberia during the Jurassic from  
762 palaeomagnetic data, *Tectonophysics*, 50, 105–120, 2010.
- 763 Page, K.N.: The Lower Jurassic of Europe: its subdivision and correlation, *Geol. Survey*  
764 *Denmark and Greeland Bull.*, 1, 23–59, 2003.
- 765 Payne, J.L. and Kump, L.R.: Evidence for recurrent Early Triassic massive volcanism  
766 from quantitative interpretation of carbon isotope fluctuations, *Earth Planet.*  
767 *Sc. Lett.*, 256, 264–277, 2007.
- 768 Price, G.D.: The evidence of polar ice during the Mesozoic, *Earth Sci. Rev.*, 48, 183–210,  
769 1999.
- 770 Price, G. D., Twitchett, R.J., Smale, C. and Marks, V.: Isotopic analysis of the life history  
771 of the enigmatic squid *Spirula spirula*, with implications for studies of fossil  
772 cephalopods, *Palaios*, 24, 273–279, 2009.
- 773 [Prokoph, A., Shields, G.A. and Veizer, J.: Compilation and time-series analysis of a](#)  
774 [marine carbonate  \$\delta^{18}\text{O}\$ ,  \$\delta^{13}\text{C}\$ ,  \$^{87}\text{Sr}/^{86}\text{Sr}\$  and  \$\delta^{34}\text{S}\$  database through Earth history.](#)  
775 [Earth Sci. Rev. 87\(3\), 113–133, 2013.](#)
- 776 Quesada, S., Robles, S. and Rosales, I.: Depositional architecture and transgressive–  
777 regressive cycles within Liassic backstepping carbonate ramps in the Basque–  
778 Cantabrian Basin, northern Spain, *J. Geol. Soc. London*, 162, 531–548, 2005.
- 779 Rees, P.A., Zeigler, A.M. and Valdes, P.J.: Jurassic phytogeography and climates: new  
780 data and model comparisons, in: *Warm climates in Earth History*, edited by  
781 Huber, B., Macleod, K., Wing, S., Cambridge University Press, Cambridge, 297–  
782 318, 1999.
- 783 Retallack, G.J.: Greenhouse crises of the past 300 million years, *Geol. Soc. Am. Bull.*,  
784 121, 1441–1455, 2009.
- 785 Rexfort, A. and Mutterlose, J.: The role of biogeography and ecology on the isotope  
786 signature of cuttlefishes (Cephalopoda, Sepiidae) and the impact on belemnite  
787 studies, *Palaeogeogr. Palaeocl.*, 244, 212–221, 2009.
- 788 Röhl, H.J., Schmid-Röhl, A., Oschmann, W., Frimmel, A. and Schwark, L.: The Posidonia  
789 Shale (Lower Toarcian) of SW-Germany: an oxygen-depleted ecosystem

- 790 controlled by sea level and palaeoclimate, *Palaeogeogr. Palaeocl.*, 165, 27–52,  
791 2001.
- 792 Rosales, I., Quesada, S. and Robles, S.: Primary and diagenetic isotopic signal in fossils  
793 and hemipelagic carbonates: the lower Jurassic of northern Spain,  
794 *Sedimentology*, 48, 1149–1169, 2001.
- 795 Rosales, I., Quesada, S. and Robles, S.: Paleotemperature variations of Early Jurassic  
796 seawater recorded in geochemical trends of belemnites from the  
797 Basque–Cantabrian basin, northern Spain, *Palaeogeogr. Palaeocl.*, 203,  
798 253–275, 2004.
- 799 Sælen, G., Doyle, P. and Talbot, M.R.: Stable-Isotope Analyses of Belemnite Rostra  
800 from the Whitby Mudstone Fm., England: Surface Water Conditions during  
801 Deposition of a Marine Black Shale, *Palaios*, 11, 97–117, 1996.
- 802 Schmid-Röhl, A., Röhl, H.J., Oschmann, W., Frimmel, A. and Schwark, L.:  
803 Palaeoenvironmental reconstruction of Lower Toarcian epicontinental black  
804 shales (Posidonia Shale, SW Germany): global versus regional control, *Geobios*,  
805 35, 13–20, 2002.
- 806 Schouten, S., van Kaam-Peters, H.M.E., Rijpstra, W.I.C., Schoell, M. and Sinninghe  
807 Damste, J.S.: Effects of an oceanic anoxic event on the stable carbon isotopic  
808 composition of Early Toarcian carbon, *Am. J. Sci.*, 300, 1–22, 2000.
- 809 Shackleton, N. J. and Kenett, J. P.: Paleotemperature history of the Cenozoic and the  
810 initiation of Antarctic glaciation: Oxygen and carbon isotope analysis in DSDP  
811 sites 277, 279 and 281, in: *Initial Reports of the Deep Sea Drilling Projects*, 29,  
812 edited by: Kennet, J. P., Houtz, R. E., Andrews, P. B., Edwards, A. R., Gosting, V.  
813 A., Hajós, M., Hampton, M. A., Jenkins, D.G., Margolis, S. V., Owenshine, A. T.,  
814 and Perch-Nielsen, K., US Government Printing Office, Washington, 743–756,  
815 1975.
- 816 Silva, R.L., Duarte, L.V., Comas-Rengifo, M.J., Mendonça Filho, J.G. and Azerêdo, A.C.:  
817 Update of the carbon and oxygen isotopic records of the Early–late  
818 Pliensbachian (Early Jurassic, ~187Ma): insights from the organic-rich  
819 hemipelagic series of the Lusitanian Basin (Portugal), *Chem. Geol.*, 283,  
820 177–184. 2011.
- 821 [Silva, R.L. and Duarte, L.V.: Organic matter production and preservation in the  
822 Lusitanian Basin \(Portugal\) and Pliensbachian climatic snaps. \*Global and Planet.  
823 Change\*, 131, 24–34. 2015.](#)
- 824 Steinhorsdottir, M. and Vajda, V.: Early Jurassic (late Pliensbachian) CO<sub>2</sub>  
825 concentrations based on stomatal analysis of fossil conifer leaves from eastern  
826 Australia, *Gondwana Res.*, 27, 829–897, 2015.
- 827 Suan, G., Mattioli, E., Pittet, B., Maillot, S. and Lécuyer, C.: Evidence for major  
828 environmental perturbation prior to and during the Toarcian (Early Jurassic)  
829 Oceanic Anoxic Event from the Lusitanian Basin, Portugal, *Paleoceanography*  
830 23, 1202, doi: 10.1029/2007PA001459, 2008.

- 831 Suan, G., Mattioli, E., Pittet, B., Lécuyer, C., Suchéras-Marx, B., Duarte, L.V., Philippe,  
832 M., Reggiani, F. and Martineau, F.: Secular environmental precursor to Early  
833 Toarcian (Jurassic) extreme climate changes, *Earth Planet. Sc. Lett.*, 290,  
834 448–458, 2010.
- 835 Suan, G., Nikitenko, B., Rogov, M.A., Baudin, F., Spangenberg, J.E., Knyazev, V.G.,  
836 Glinskikh, L.A., Goryacheva, A.A., Adatte, T., Riding, J., Föllmi, K.B., Pittet,  
837 B., Mattioli, E. and Lécuyer, C.: Polar record of Early Jurassic massive carbon  
838 injection, *Earth Planet. Sc. Lett.*, 312, 102–113, 2011.
- 839 Suárez-Vega, L.C.: *Estratigrafía del Jurásico en Asturias*, *Cuad. Geol. Ibérica*, 3, 1–369,  
840 1974.
- 841 Svensen, H., Planke, S., Chevalier, L., Malthe-Sørensen, A., Corfu, F. and Jamtveit, B.:  
842 Hydrothermal venting of greenhouse gasses triggering Early Jurassic global  
843 warming, *Earth Planet. Sc. Lett.*, 256, 554–566, 2007.
- 844 Ullmann, C.V. and Korte, C.: Diagenetic alteration in low-Mg calcite from microfossils:  
845 a review, *Geol. Q.*, 59, 3–20, 2015.
- 846 Ullmann, C.V., Thibault, N., Ruhl, M., Hesselbo, S.P. and Korte, C.: Effect of a Jurassic  
847 oceanic anoxic event on belemnite ecology and evolution, *P. Nat. Acad. Sci.*  
848 *USA*, 111, 10073–10076, 2014.
- 849 Valenzuela, M.: *Estratigrafía, sedimentología y paleogeografía del Jurásico de Asturias*,  
850 Ph. D. Thesis, Fac. Sci. Geol. Univ. Oviedo, Spain, 1988.
- 851 van de Schootbrugge, Harazim, D., Sorichter, K., Oschmann, W., Fiebig, J., Püttmann,  
852 W., Peinl, M., Zanella, F., Teichert, B.M.A., Hoffmann, Stadnitskaia, J.A. and  
853 Roshental, Y.: The enigmatic ichnofossil *Tisoa siphonalis* and widespread  
854 authigenic seep carbonate formation during the Late Pliensbachian in southern  
855 France, *Biogeosciences*, 7, 3123–3138, doi: 10.5194/bg-7-3123-2010, 2010.
- 856 **Wierzbowski, H. and Joachimski, M.M.: Reconstruction of Late Bajocian–Bathonian**  
857 **marine palaeoenvironments using carbon and oxygen isotope ratios of**  
858 **calcareous fossils from the Polish Jura Chain (central Poland). *Palaeogeogr.***  
859 ***Palaeocli.*, 254, 523–540, 2007.**
- 860 Wigley, T.M.L., Richels, R. and Edmonds, J.A.: Economic and environmental choices in  
861 the stabilization of atmospheric CO<sub>2</sub> concentrations, *Nature*, 379, 240–243,  
862 1996.
- 863 Woodfine, R.G., Jenkyns, H.C., Sarti, M., Baroncini, F. and Violante, C.: The response of  
864 two Tethyan carbonate platforms to the early Toarcian (Jurassic) oceanic anoxic  
865 event: environmental change and differential subsidence, *Sedimentology*, 55,  
866 1011–1028, 2008.
- 867 Zakharov, V.A., Shurygin, B.N., Il'ina, V.I. and Nikitenko, B.L.: Pliensbachian–Toarcian  
868 biotic turnover in North Siberia and the Arctic Region, *Stratigr. Geol. Correl.*, 14,  
869 399–417, 2006.

870

871

872 **FIGURE CAPTIONS**

873 Fig. 1. Location maps of the Rodiles section. (a): Sketched geological map of Iberia  
874 showing the position of the Asturian Basin. (b): Outcrops of the Jurassic deposits in the  
875 Asturian and the western part of the Basque–Cantabrian basins, and the position of  
876 the Rodiles section. (c): Geological map of the Asturian Basin showing the distribution  
877 of the different geological units and the location of the Rodiles section.

878 Fig. 2. Thick sections photomicrographs of some of the belemnites sampled for stable  
879 isotope analysis from the Upper Sinemurian and Pliensbachian of the Rodiles section.  
880 The unaltered by diagenesis non luminescent sampling areas (SA), where the samples  
881 have been collected, are indicated. A and B Sample ER 351, Late Sinemurian  
882 *Raricostatum* Chronozone, *Aplanatum* Subchronozone. A: optical transmitted light  
883 microscope, showing the carbonate deposit filling the alveolous (Cf), the outer rostrum  
884 cavum wall (Cw) and fractures (Fr). B: cathodoluminescence microscope  
885 photomicrograph, showing luminescence in the carbonate deposit filling the alveolous  
886 (Cf), in the outer rostrum cavum wall (Cw) and in the fractures (Fr). SA represents the  
887 unaltered sampling area. C and D: Sample ER 337, Early Pliensbachian *Jamesoni*  
888 Chronozone, *Taylori*-*Polymorphus* Subchronozones. C: optical transmitted light  
889 microscope, showing fractures (Fr). D: cathodoluminescence microscope  
890 photomicrograph, showing luminescence in stylolites (St). SA is the unaltered sampling  
891 area. E and F: Sample ER 589a Early Pliensbachian *Margaritatus* Chronozone,  
892 *Subnodosus* Subchronozone. E: cathodoluminescence microscope, showing  
893 luminescence in the apical line (Ap), fractures (Fr) and stylolites (St). This area of the  
894 section was not suitable for sampling. F: another field of the same sample as H  
895 showing scarce fractures (Fr) and the unaltered not luminescent sampled area (SA). G  
896 and H: Sample ER 549a, Late Pliensbachian *Margaritatus* Chronozone, *Stokesi*  
897 Subchronozone. G: cathodoluminescence microscope showing luminescent growth  
898 rings (Gr) and stylolites (St). Area not suitable for sampling. H: cathodoluminescence  
899 microscope photomicrograph, of the same sample as G, showing luminescent growth  
900 rings (Gr) and fractures (Fr), with unaltered sampling area (SA). I: Sample ER 555 Late  
901 Pliensbachian *Margaritatus* Chronozone, *Stokesi* Subchronozone.  
902 Cathodoluminescence microscope photomicrograph showing luminescent growth rings  
903 (Gr) and the unaltered sampling area (SA). J and K: Sample ER 623 Late Pliensbachian  
904 *Spinatum* Chronozone, *Apyrenum* Subchronozone. J: cathodoluminescence  
905 microscope photomicrograph showing luminescent stylolites (St). K: Another field of  
906 the same sample as J showing luminescence in the apical line (Ap) and fractures (Fr) as  
907 well as the non luminescent unaltered sampling area (SA). L: Sample ER 597, Late  
908 Pliensbachian *Margaritatus* Chronozone, *Gibbosus* Subchronozone.  
909 Cathodoluminescence microscope photomicrograph showing luminescent carbonate  
910 deposit filling the alveolous (Cf), the outer and inner rostrum cavum wall (Cw), the  
911 fractures (Fr) and the non luminescent sampling area (SA). Scale in bar for all the  
912 photomicrographs: 1mm.

913

914 Fig. 3. Cross-plot of the  $\delta^{18}\text{O}_{\text{bel}}$  against the  $\delta^{13}\text{C}_{\text{bel}}$  values obtained in the Rodiles section  
915 showing a cluster type of distribution. All the assayed values are within the rank of  
916 normal marine values, and the correlation coefficient between both stable isotope  
917 values is negative, supporting the lack of diagenetic overprints in the sampled  
918 belemnite calcite.  $\delta^{18}\text{O}_{\text{bel}}$  and  $\delta^{13}\text{C}_{\text{bel}}$  in PDB.

919

920 Fig 4. Sketch of the stratigraphical succession of the uppermost Triassic and the  
921 Jurassic deposits of the Asturian Basin. The studied interval corresponds to the lower  
922 part of the Santa Mera Member of the Rodiles Formation. Pli.=Pliensbachian, Toar.=  
923 Toarcian. Aal.= Aalenian. Baj.=Bajocian.

924

925 Fig. 5. Stratigraphical succession of the Upper Sinemurian, the Pliensbachian and the  
926 Lower Toarcian deposits of the Rodiles section, showing the lithological succession, the  
927 ammonite taxa distribution, as well as the profiles of the  $\delta^{18}\text{O}_{\text{bel}}$  and  $\delta^{13}\text{C}_{\text{bel}}$  values  
928 obtained from belemnite calcite.  $\delta^{18}\text{O}_{\text{bel}}$  and  $\delta^{13}\text{C}_{\text{bel}}$  in PDB. Chronozones  
929 abbreviations: TEN: Tenuicostatum. Subchronozones abbreviations: RA: Raricostatum.  
930 MC: Macdonnelli. AP: Aplanatum. BR: Brevispina. JA: Jamesoni. MA: Masseanum. LU:  
931 Luridum. MU: Maculatum. CA: Capricornus. FI: Figulinum. ST: Stokesi. HA:  
932 Hawskerense. PA: Paltum. SE: Semicelatum. EL: Elegantulum. FA: Falciferum.

933

934 Fig. 6. Correlation chart of the belemnite calcite-based  $\delta^{13}\text{C}$  sketched curves across  
935 Western Europe. The earliest isotopic event is the **Late** Sinemurian  $\delta^{13}\text{C}$  positive  
936 excursion, followed by the **Early** Pliensbachian negative excursion and the Ibex–Davoei  
937 positive peak. The **Late** Pliensbachian  $\delta^{13}\text{C}$  positive excursion is bounded by a  $\delta^{13}\text{C}$   
938 negative peak, located around the Pliensbachian–Toarcian boundary. A significant  $\delta^{13}\text{C}$   
939 positive excursion is recorded in the **Early** Toarcian.  $\delta^{13}\text{C}_{\text{bel}}$  values in PDB. .  
940 Chronozones abbreviations: TEN: Tenuicostatum. SER: Serpentinum.

941

942 Fig. 7. Curve of seawater palaeotemperatures of the **Late** Sinemurian, Pliensbachian  
943 and Early Toarcian, obtained from belemnite calcite in the Rodiles section of Northern  
944 Spain. Two warming intervals corresponding to the **Late** Sinemurian and the **Early**  
945 Pliensbachian are followed by an important cooling interval, developed at the Late  
946 Pliensbachian, as well as a (**super**)warming event recorded in the Early Toarcian.  
947 Chronozones abbreviations: RAR: Raricostatum. D: Davoei. TENUICOSTA.:  
948 Tenuicostatum. Subchronozones abbreviations: DS: Densinodulum. RA: Raricostatum.  
949 MC: Macdonnelli. AP: Aplanatum. BR: Bevispina. JA: Jamesoni. VA: Valdani. LU: Luridum.  
950 CA: Capricornus. FI: Figulinum. SU: Subnodosus. PA: Paltum. SE: Semicelatum. FA:  
951 Falciferum.

952

953 Fig. 8. Correlation chart of the belemnite calcite-based  $\delta^{18}\text{O}$  sketched curves obtained  
954 in different areas of Western Europe. Several isotopic events along the **latest**  
955 Sinemurian, Pliensbachian and **Early** Toarcian can be recognized. The earliest event is a  
956  $\delta^{18}\text{O}$  negative excursion corresponding to the **Late** Sinemurian Warming. After an  
957 interval of “normal”  $\delta^{18}\text{O}$  values developed in most of the Jamesoni Chronozone and  
958 the **earliest** part of the Ibex Chronozone, another  $\delta^{18}\text{O}$  negative excursion was  
959 developed in the Ibex, Davoei and **earliest** Margaritatus chronozones, representing the  
960 **Early** Pliensbachian Warming interval. A main  $\delta^{18}\text{O}$  positive excursion is recorded at the  
961 **Late** Pliensbachian and the **earliest** Toarcian in all the correlated localities,  
962 representing the important **Late** Pliensbachian Cooling interval. Another prominent  
963  $\delta^{18}\text{O}$  negative shift is recorded in the Early Toarcian. Values are progressively more  
964 negative in the Tenuicostatum Chronozone and suddenly decrease around the  
965 Tenuicostatum–Serpentinum zonal boundary, delineating the **Early** Toarcian  $\delta^{18}\text{O}$   
966 negative excursion which represents the **Early** Toarcian (super)Warming interval.  
967  $\delta^{18}\text{O}_{\text{bel}}$  values in PDB.



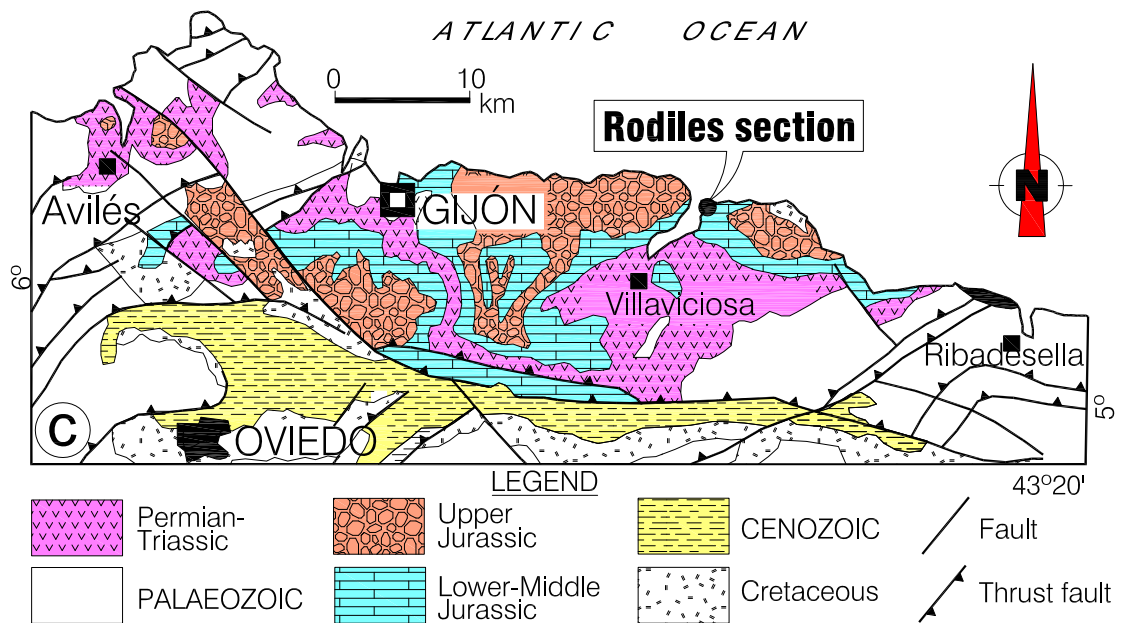
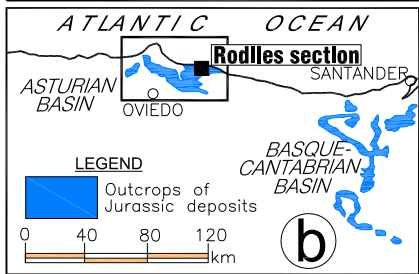
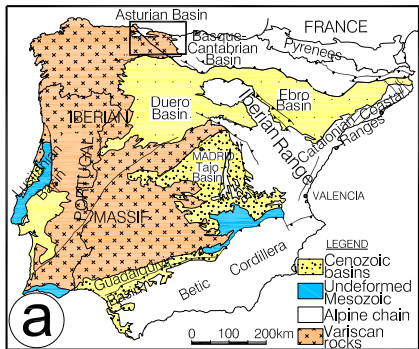


Fig. 1. Gómez, Comas-Rengifo and Goy

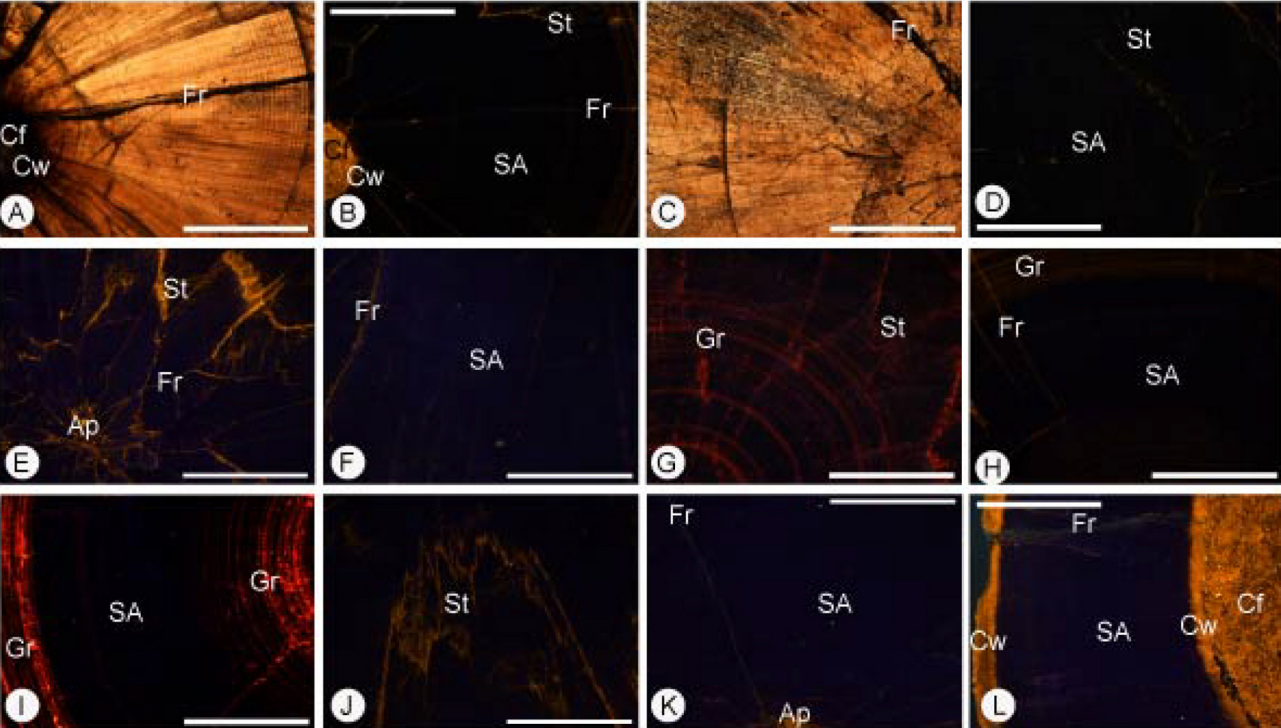


Fig 2. Gómez, Comas and Goy

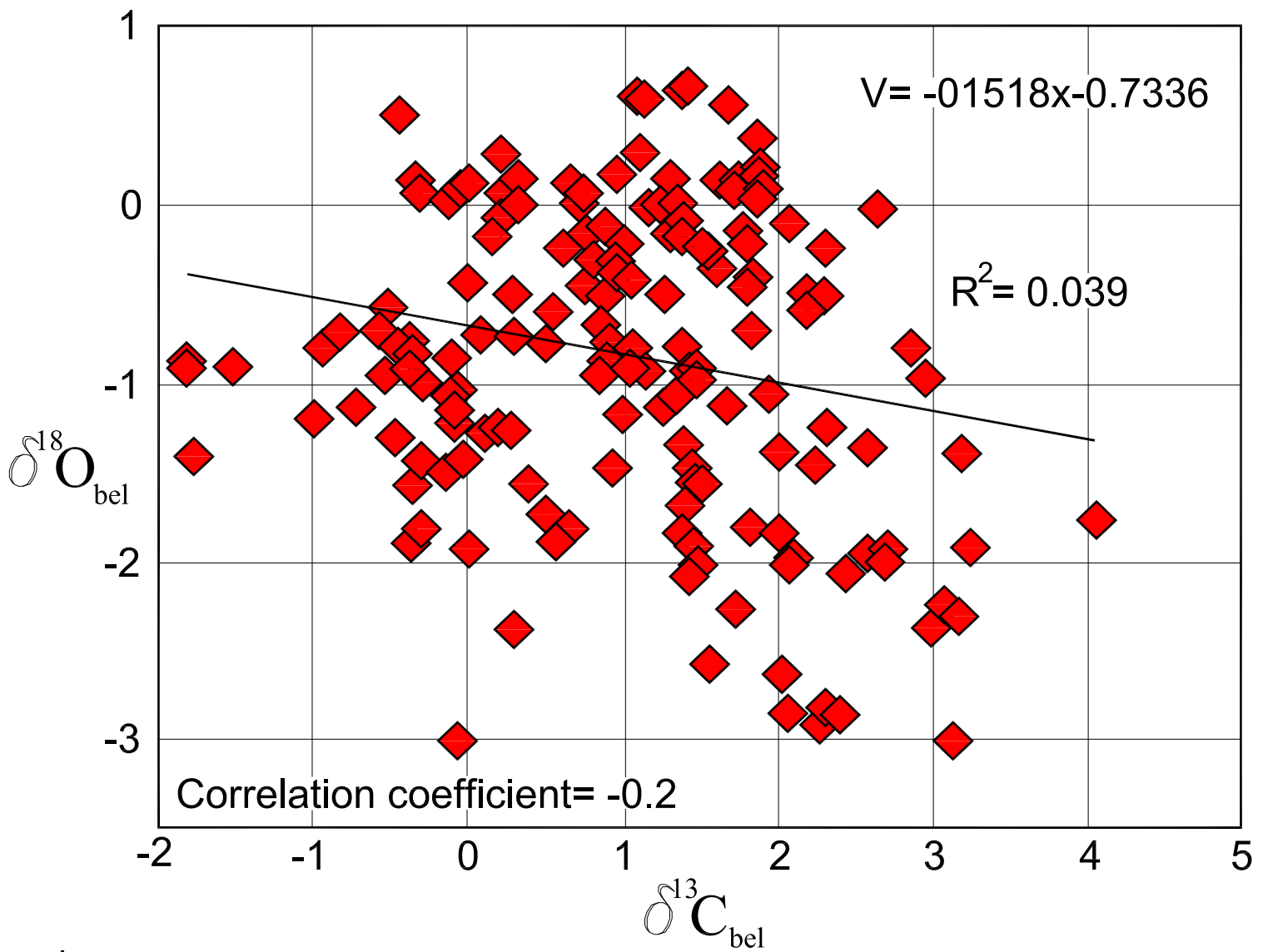


Fig. 3. Gómez, Comas-Rengifo and Goy

STUDIED  
INTERVAL

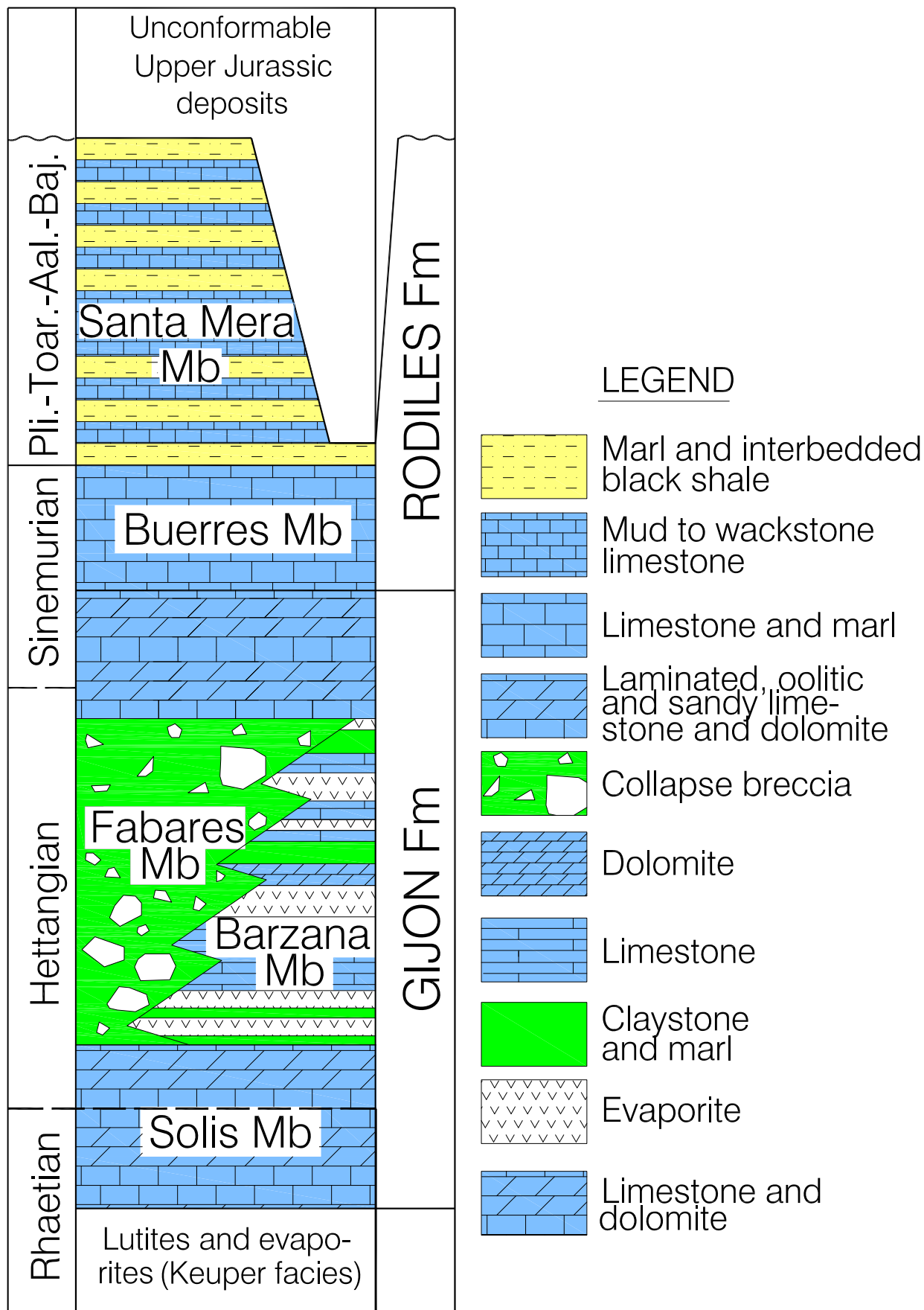


Fig. 4. Gómez, Comas-Rengifo and Goy

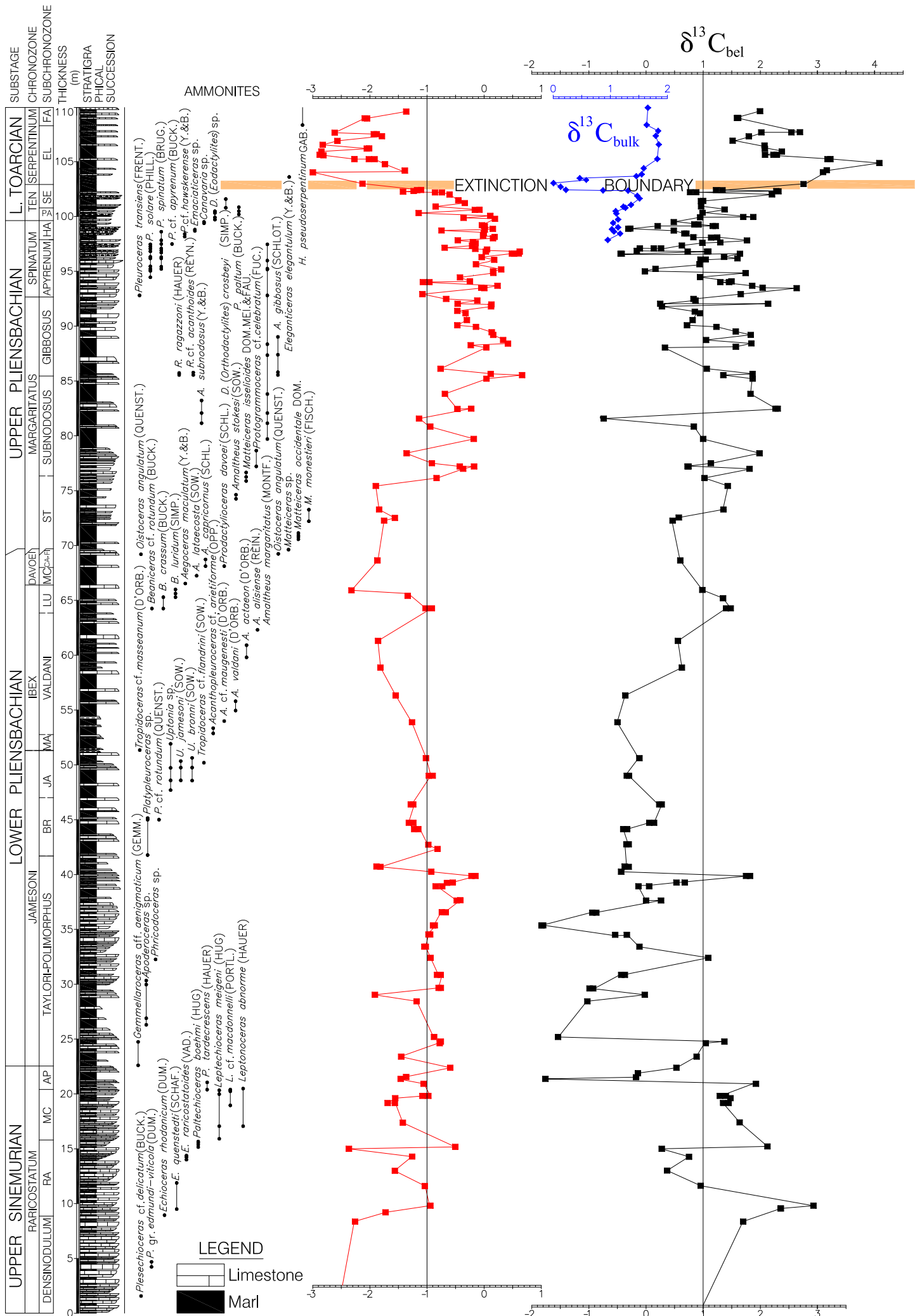


Fig. 5. Gómez, Comas-Rengifo and Goy

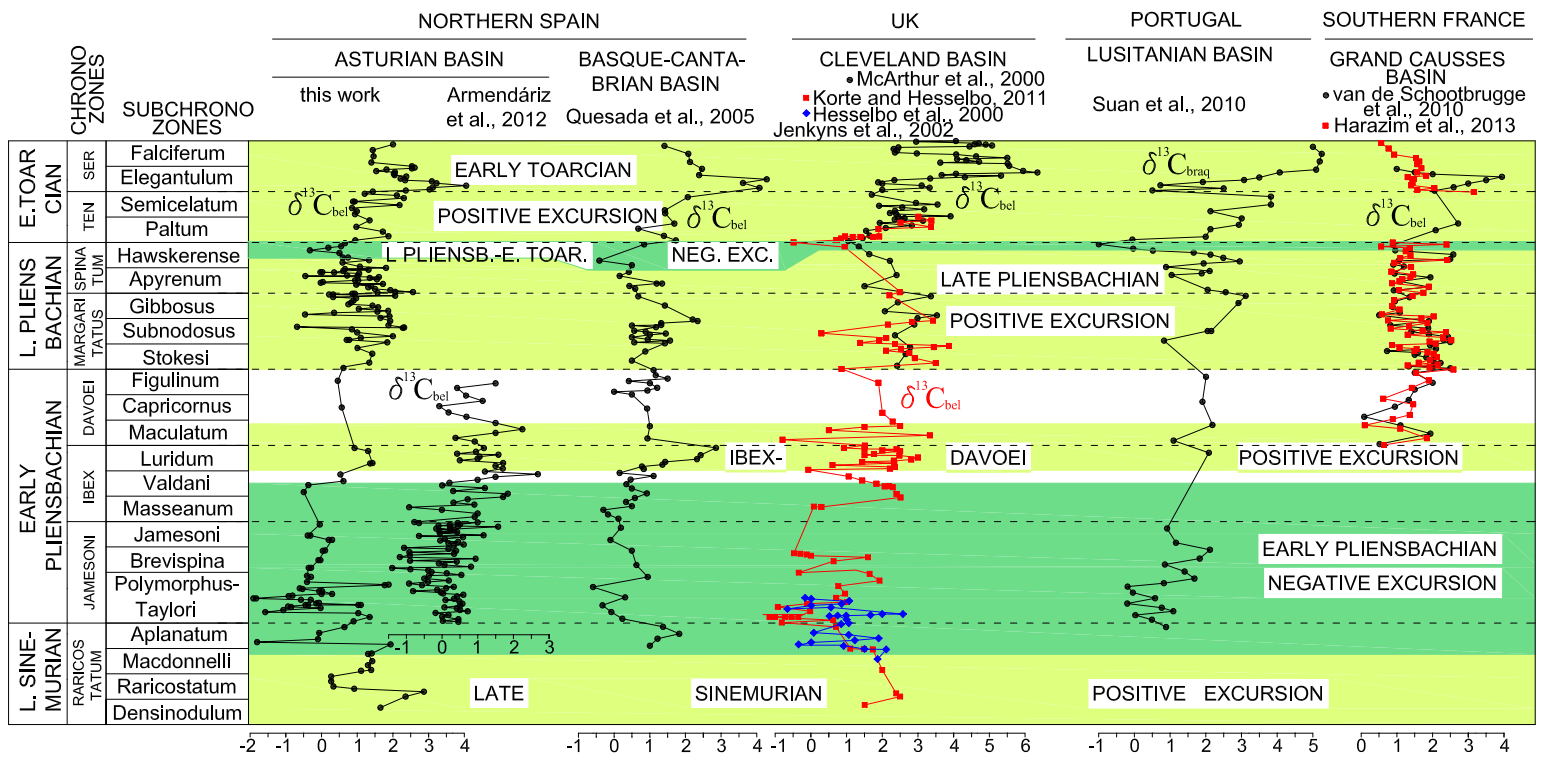


Fig. 6. Gómez, Comas-Rengifo and Goy

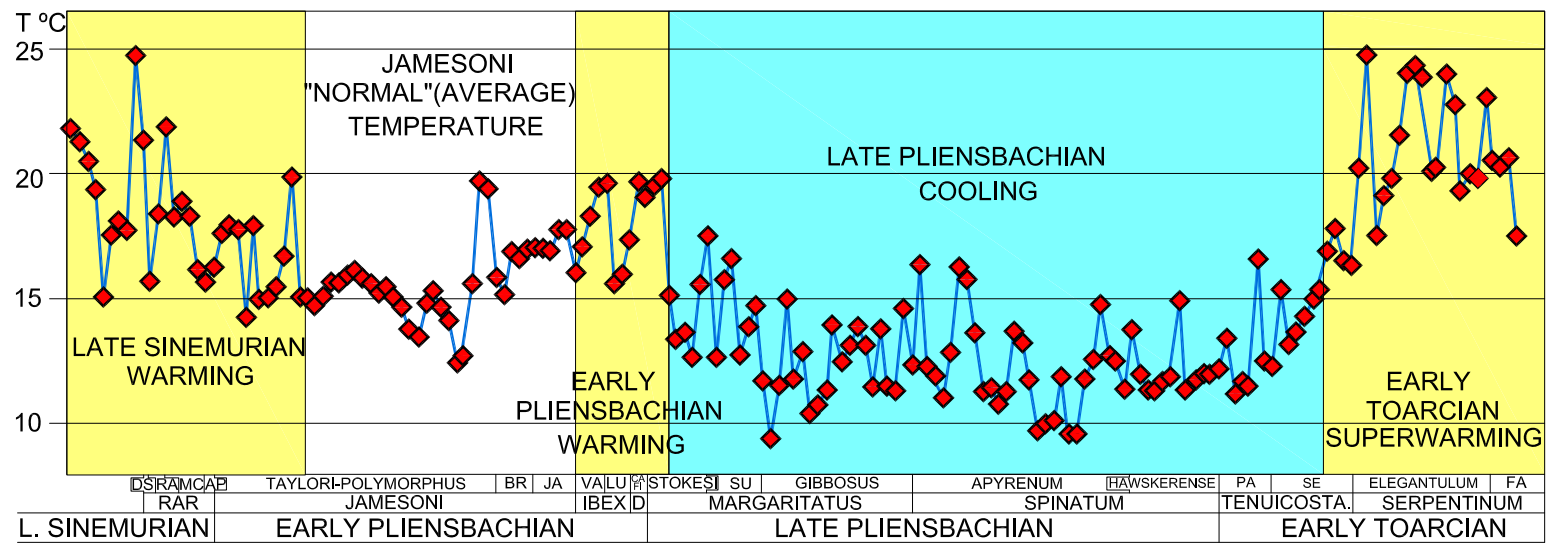


Fig. 7. Gómez, Comas-Rengifo and Goy

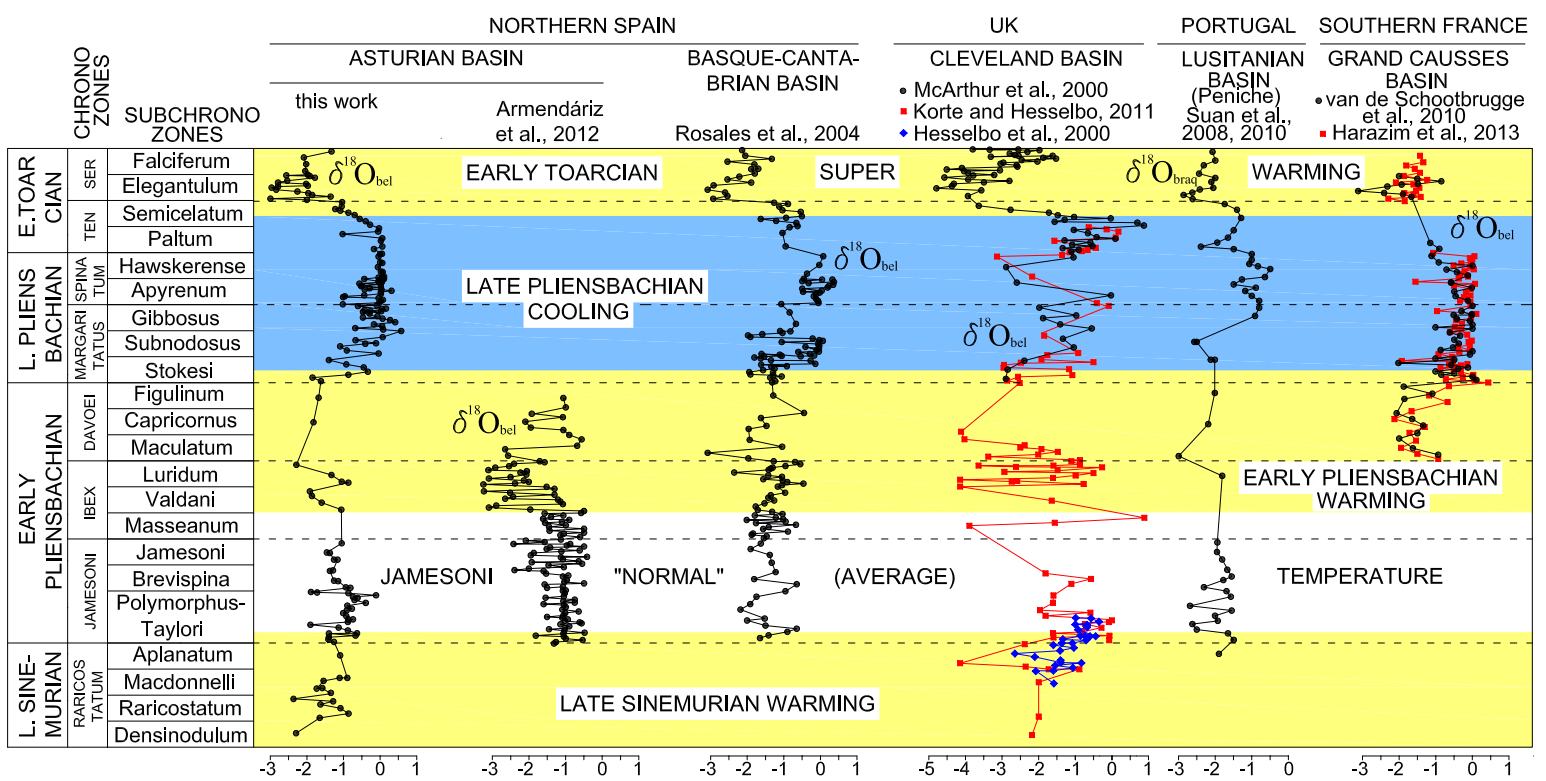


Fig. 8. Gómez, Comas-Rengifo and Goy